Award Number: **W81XWH-18-1-0322**

TITLE: **Targeting Cardiac Calcium Regulation and Fibrosis in DMD Models**

PRINCIPAL INVESTIGATOR: **Jeong, Dongtak, PhD**

CONTRACTING ORGANIZATION: **Icahn School of Medicine at Mount Sinai**

REPORT DATE: **Sept 2020**

TYPE OF REPORT: **Annual**

PREPARED FOR: U.S. Army Medical Research and Materiel Command
Fort Detrick, Maryland 21702-5012

DISTRIBUTION STATEMENT: Approved for Public Release;
Distribution Unlimited

REPORT DOCUMENTATION PAGE

Form Approved
OMB No. 0704-0188

1. REPORT DATE *(DD-MM-YYYY)*	**2. REPORT TYPE**	**3. DATES COVERED** *(From - To)*
Sept 2020	Annual	15 Aug 2019 - 14 Aug 2020

4. TITLE AND SUBTITLE
Targeting Cardiac Calcium Regulation and Fibrosis in DMD Models

5a. CONTRACT NUMBER

5b. GRANT NUMBER
W81XWH-18-1-0322

5c. PROGRAM ELEMENT NUMBER

6. AUTHOR(S)
Dongtak Jeong

5d. PROJECT NUMBER

5e. TASK NUMBER

5f. WORK UNIT NUMBER

7. PERFORMING ORGANIZATION NAME(S) AND ADDRESS(ES)

ICAHN SCHOOL OF MEDICINE AT
MOUNT SINAI
ONE GUSTAVE L LEVY PL
NEW YORK NY 10029-6504

8. PERFORMING ORGANIZATION REPORT NUMBER

9. SPONSORING / MONITORING AGENCY NAME(S) AND ADDRESS(ES)
U.S. Army Medical Research and
Material Command
Fort Detrick, Maryland
21702-5012

10. SPONSOR/MONITOR'S ACRONYM(S)

11. SPONSOR/MONITOR'S REPORT NUMBER(S)

12. DISTRIBUTION / AVAILABILITY STATEMENT
Approved for public release; distribution unlimited

13. SUPPLEMENTARY NOTES

14. ABSTRACT
Cardiomyopathy is a prominent feature of Duchenne Muscular Dystrophy (DMD) with increased intracellular Ca^{2+} and significant interstitial fibrosis being major pathophysiological hallmarks. miRNA-25 has been identified as a suppressor of both SERCA2a and Smad7 in several experimental animal models. In Phase I, we united miR-25 TuD with AAV9, in order to assess the effect of miR-25 inhibition on cardiac function in aged dystrophin/utrophin (MDX/UTRN) KO mice which is a validated transgenic murine model for DMD. We found that AAV9 miR-25 TuD transfer resulted in the strong and stable inhibition of cardiac miR-25 levels. This resulted in increased SERCA2a and Smad7 expression and in turn improved cardiac function, decreased cardiac fibrosis, and also lead to a significantly improved survival rate. In Phase II, we generated new AAV vectors with various promoters to obtain tissue specific expression and minimize off-target effect. Conclusively, we could achieve a better tissue specificity using these promoters but there is clear imitation using current AAV constructs in terms of the intensity of target gene expression, which should be addressed in further studies.

15. SUBJECT TERMS
DMD, miRNA-25, Tough Decoy (TuD), SERCA2a, Smad7, Cardiomyopathy, Troponin T, Periostin, Fibrosis, Exosome, CCN5

16. SECURITY CLASSIFICATION OF:			**17. LIMITATION OF ABSTRACT**	**18. NUMBER OF PAGES**	**19a. NAME OF RESPONSIBLE PERSON**
a. REPORT	**b. ABSTRACT**	**c. THIS PAGE**			USAMRMC
U	U	U	UU	42	**19b. TELEPHONE NUMBER** *(include area code)*

TABLE OF CONTENTS

1. INTRODUCTION:

Heart disease profoundly affects the quality of life of Duchenne Muscular Dystrophy (DMD) patients. DMD is caused by mutations in the dystrophin gene [1,2], which anchors the cytoskeleton, sarcolemma, and extracellular matrix (ECM) together to prevent cell membrane damage during muscle contraction. However, abnormal dystrophin expression weakens the link between the ECM and the cytoskeleton [3] resulting in affected muscle cells degenerating and necrotizing. Until recently, DMD patients life span was determined mostly by respiratory failure, with approximately 80% to 90% of DMD deaths [4-7]. With improved respiratory care, death by cardiomyopathy has become more frequent, even approaching 40% in some studies [8]. Additionally, myocardial fibrosis is the second leading cause of death in DMD [6,7,9,10], occurring in more than 96% of DMD hearts. Fibrotic lesions cause fatal ventricular arrhythmias in DMD patients [7,11,12]. Although further research to clarify molecular mechanisms underlying dystrophin-deficient heart disease remains, evidence suggests that abnormal elevation of cytosolic calcium is central to the pathogenesis of DMD heart disease [13-17].

The sarcoplasmic reticulum is the primary calcium storage organelle in muscle cells. In CMs, removal of cytosolic calcium is mainly accomplished by the cardiac isoform of sarcoplasmic reticulum calcium ATPase (SERCA2a) via its pump activity [18]. SERCA2a expression/activity is reduced in various forms of heart failure (HF) in experimental animal models and human patients [19,20]. Additionally, aged mdx models show decrease in endogenous SERCA2a expression, which was restored by SERCA2a gene transfer [21]. Furthermore, in mdx/utrophin double KO mice, which recapitulate human DMD pathophysiology, SERCA2a expression was found to be significantly decreased. Recently our group has found additional mechanisms to fine-tune SERCA2a post-transcriptionally through microRNAs (miRs). These small non-coding RNAs regulate protein expression by destabilization and/or translational inhibition of target messenger RNAs (mRNAs). Like mRNAs, expression of miRs is regulated in HF including cardiomyopathy [22-25]. Advances in understanding the molecular mechanisms that are associated with pathological stress have offered numerous important CM specific targets for intervention [23]. Specifically, miR-25 has consistently been identified as a potent regulator of SERCA2a and showed anti-miR-25 treatment enhanced cardiac contractility and function through SERCA2a restoration in murine HF models [26]. Furthermore, *in silico* and *in vitro* experiments confirmed that miR-25 has an additional binding partner, SMAD7. SMAD7 is an endogenous antagonist of TGF-β signaling, a common pro-fibrotic pathway in many organs including the heart.

With the ultimate goal to enhance cardiac function in DMD patients, a stable and efficient delivery of antagonizing molecule against miR-25 is necessary. An inhibitory construct against miR-25, so-called miR-25 tough decoy, was successfully generated. It improved cardiac function and significantly reduced cardiac fibrosis in TAC-induced HF mouse model (*paper in revision*). This construct was combined with the traditionally used AAV9, a cardiac serotype, for gene therapy treatments [27]. However, there are still limitations which include off-target expression such as liver tropism [28,29]. Transcriptional regulation has been used to address these issues. Our approach will use a *cis*-acting regulatory module sequence [30] to improve cardiac specificity and enhance expression. Additionally, two different promoters, periostin[31] and troponin-T[32], will be used to target MFBs and CMs, respectively.

2. KEYWORDS:

DMD, miRNA-25, Tough Decoy (TuD), SERCA2a, Smad7, Cardiomyopathy, Troponin T, Periostin, Fibrosis, Exosome, CCN5

3. ACCOMPLISHMENTS:

1) What were the major goals of the project?

Since our group found that anti-miR-25 treatment enhanced cardiac contractility and function through SERCA2a restoration in murine HF models[26], an efficient and stable antagonism of miR-25 has been found, miR-25 TuD. Furthermore, we found that miR-25 has an addition binding partner, SMAD7. SMAD7 has been found to inhibit fibrosis through the TGF-β signaling pathway. Since cardiac complications that arise in chronic DMD patients are related to cardiac dysfunction and fibrosis, we hypothesize that miR-25 TuD will ameliorate these phenotypes and improve the quality of life of DMD patients. Furthermore, we will enhance the tissue-specific expression of miR-25 TuD using a cell type specific promoter and minimize off-target effect.

Proposed speficic aims;

Specific aim 1: Therapeutic evaluation of miR-25 TuD on cardiac function and fibrosis.
Preliminary data have shown that antagonizing miR-25 had a beneficial effect on HF animal model through the regulation of SERCA2a expression. Moreover, we have recently identified an additional binding partner, SMAD7, an endogenous antagonist of TGF-β signaling pathway, which is a major signaling pathway in cardiac fibrosis. Therefore, we will apply miR-25 TuD in DMD mouse model and evaluate the efficacy and efficiency in terms of cardiac function and fibrosis.

Specific aim 2: Therapeutic evaluation of miR-25 TuD using cell type specific promoters.
AAV9 is a widely used serotype for cardiac gene therapy [27]. However, there are still limitations including off-target expression such as liver tropism [28,29]. Since we have identified that miR-25 has dual targets in the heart, we will apply two independent promoters for individual cell types (CMs and cardiac MFBs). AAV vectors have traditionally been used with the CMV promoter due to its high expression efficiency. Although cardiac specific promoters such as TnT exist, they have low expression profiles. Recently, we combined TnT with an Enh and achieved substantially high expression of the gene of interest, comparable to that of CMV, with minimal off-target expression. Therefore, we will apply this with miR-25 TuD in terms of cardiac functional study. On the other hand, to target cardiac fibrosis, which occurs mainly by proliferation of residential CF [31], a Postn promoter will be applied, which is exclusively expressed in pathological cardiac fibrosis.

Proposed SOW for the second year of funding period;

Training-Specific Tasks: *(only applicable to training award mechanisms)*

Major Task 2: Development of cell type specific promoter with miR-25 TuD in an AAV9 vector	Months	Achievements
Subtask 1: Development of AAV construct containing Troponin T (TnT) promoter with cis-elementary module (aka enhancer (Enh)) for cardiomyocyte specific expression of miR-25 TuD	14-15	**Completed.**
Subtask 2: Development of AAV construct containing Periostin (Postn) promoter with cis-elementary module (aka enhancer (Enh)) for cardiac myofibroblast specific expression of miR-25 TuD	15-16	**Completed.**
Subtask 3: Evaluation of cis-regulatory module with TnT promoter in cardiomyocyte specificity (20 mice per group x 2 groups = 40 mice total)	17-20	**Completed.**
Subtask 4: Evaluation of cis-regulatory module with Periostin (Postn) promoter in myofibroblasts specificity	21-24	**40%** **Completed.**

(20 mice per group x 2 groups = 40 mice total)		**Delayed due to COVID-19 outbreak.**
Subtask 5: Characterize the biodistribution for miR-25 expression (20 mice per group x 2 groups = 40 mice total)	23-24	**40%** **Delayed due to COVID-19 outbreak.**
Subtask 6: Comparison between ubiquitous CMV promoter with newly generated tissue specific promoters (20 mice per group x 2 groups = 40 mice total)	21-24	**40%** **Completed.** **Delayed due to COVID-19 outbreak.**
Milestone(s) Achieved: Characterization of effects of cell type specific promoter with enhancer in terms of miR-25 expression and cardiac function	24	**80% completed.** **Delayed due to COVID-19 outbreak.** **It can be completed for next 6 months.**

2) What was accomplished under these goals?

Subtask 1: Development of AAV construct containing Troponin T (TnT) promoter with cis-elementary module (aka enhancer (Enh)) for cardiomyocyte specific expression of miR-25 TuD

- AAV construct containing Enh-TnT promoter has been successfully generated.
- DNA sequencing confirmed the orientation and mutation on DNA construct, which are shown below.
- Result

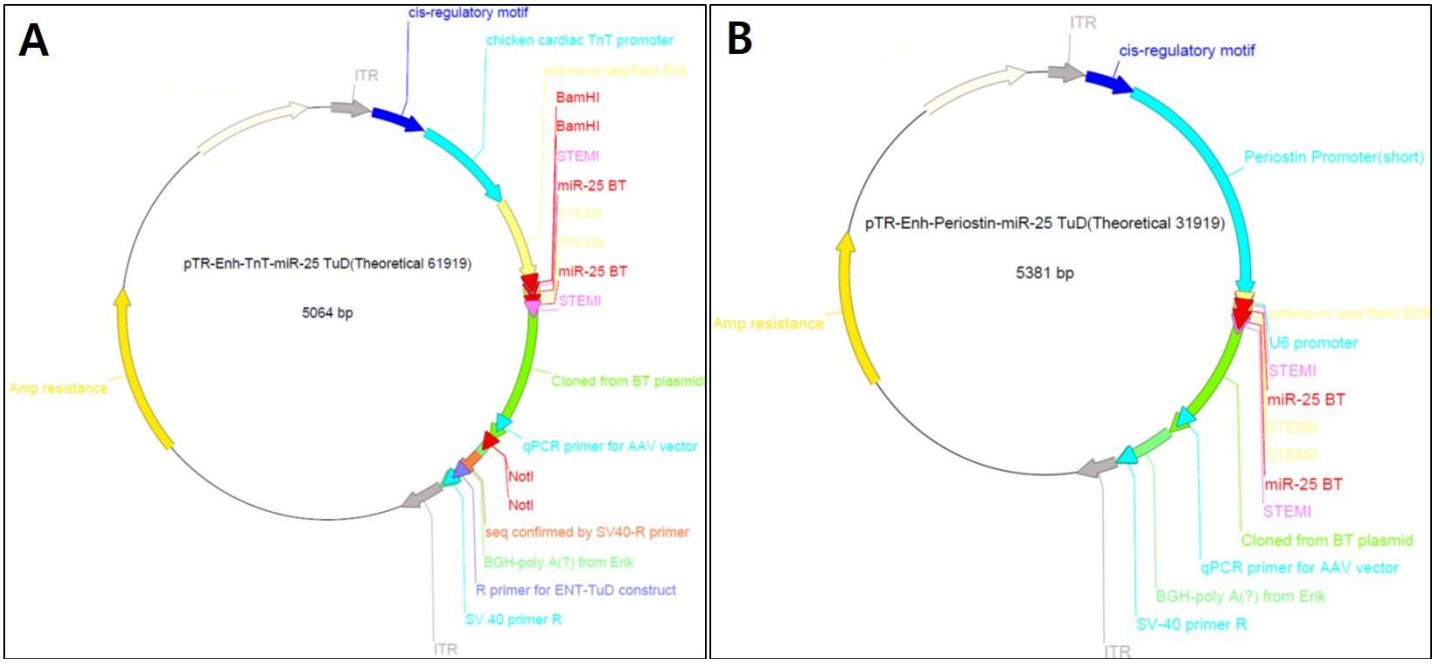

C TnT promoter (406bps)

GCAGTCTGGGCTTTCACAAGACAGCATCTGGGGCTGCGGCAGAGGGTCGGGTCCGAAGCGCTGCCTTATCAGC
GTCCCCAGCCCTGGGAGGTGACAGCTGGCTGGCTTGTGTCAGCCCCTCGGGCACTCACGTATCTCCGTCCGACGG
GTTTAAAATAGCAAAACTCTGAGGCCACACAATAGCTTGGGCTTATATGGGCTCCTGTGGGGGAAGGGGGAGCA
CGGAGGGGGCCGGGGCCGCTGCTGCCAAAATAGCAGCTCACAAGTGTTGCATTCCTCTCTGGGCGCCGGGCAC
ATTCCTGCTGCTCTGCCCGCCCCGGGGTGGGCGCCGGGGGGACCTTAAAGCCTCTGCCCCCCAAGGAGCCCTTC
CCAGACAGCCGCCGGCACCCACCGCTCCGTGGGACCT

Periostin promoter (1064bps)

GGCTTCACAACACAGCACAGAAAACACCCCCCTCTCTAGAGATGCTTTAAAATGTGTGCATTCACAGAGACTGAT
GGCTGTTTCCATTCCTTGCCAACTGAAGCTTCGTATCTTCGCAGCTTCTTCATCGAAAGGTTTCTCTGCATCTCATAT
CTGGTCATGTGTGAAGACCTAAAAAACAAACAAAAAACAAAAAAACAAAAAAACAAAGTGTCTTCCCTCAGCTA
AGAATGCTGAGGTTCAACTCCAAGAGAGTACAGTTGTTCTTACAGAAAGCAGAAGGATACTCTTGGCAGCAACC
CTGTTTCTTAATATGCATTTAATTGCCACATTATTTCTGGATTAGTAATACTTGTTTCCAGGGCTTATCAGAGTATGCA
GTGTGTGTGTAATGGAAAACAAAAAAAAGTAAAATTGTGAGAAAGATAGATAGATAGATAGATAGATAGATA
GATAGATAGATATATTTCAAAAGTTAGAGAAATTCTCCCAAAGTAGATCTTTGTTACTTAACCCTCTATACTCATTAT
GAGTTGAAAAGACATGGCCCCAGTTTCATAGGACTTCAAGGGGCATGTGTCTCTTCCACATAAGCTGTGGAAATC
ACACTTTAAATGCATTGTACATCTATCCAGGATTTGGGTTAAATGCCCCTGTGATTTCTCTTCTCCGTGTTCTGCTGT
GGAGTGATTTAAGTGCAATCAGATCAAACCAGGAAAGTAACTGAGCTCAGAGACACAGAGTGTGGTGGCAGAG
ACAGAAGGCAGAGAGATCCCTAAACTCAGAATCAGCTCTTTTCGCAATGTAAACCTATAGAAGTGAAAAACGGG
CTCACCATGATTGAAAACAAATAGGAGACAGAGTTCAGATTGCTCAGAACCCAGGAGATTTCCAGGGACAGCCC
AGGGCTGCTGGTGCTTCTGTAAGGCCATCGCAAGCTTCAGGTTGGCCCAGCGCCCCCTCCCACAGCCTTGCTCCC
TCCCACAGCCCAGAGCTATATAAACTCAGCTCTCCAGAGCACAGGCCAGATCTCTTCCTGGACGGAGCTCAGGG
CTGAAGA

Figure 1. DNA constructs for AAV9 Enh-TnT/ Enh-Postn-miR-25 TuD.

A. AAV9 Enh-TnT-miR-25 TuD plasmid map B. AAV9 Enh-Postn-miR-25 TuD plasmid map C. DNA sequences for Troponin T and Periostin promoters

Subtask 2: Development of AAV construct containing Periostin (Postn) promoter with cis-elementary module (aka enhancer (Enh)) for cardiac myofibroblast specific expression of miR-25 TuD

- AAV construct containing Enh-Postn promoter has been successfully generated.
- All confirmed DNA sequencing data are shown in Figure 1.

Subtask 3: Evaluation of cis-regulatory module with TnT promoter in cardiomyocyte specificity.

- AAV viral vectors for 40 mice were successfully produced by Jan, 2020, which are shown in Figure 2.
- **Method**

  AAV9 Enh-TnT and Enh-Postn TuD production

  Self-complementary AAV (serotype 9) constructs were generated using the pds-AAV2-EGFP vector and the optimal TuD sequence against human miRNA-25, which was kindly donated by Dr. Brian Brown, an associate professor of Genetics in the Icahn School of Medicine at Mount Sinai. The specificity of the miR-25 TuD was determined through a pMirTarget vector containing SERCA2a 3'-UTR under luciferase. The eGFP sequence was removed from the AAV construct due to viral packaging constraints. The recombinant AAV was produced by transfecting 293 T cells as described previously [34]. The AAV particles in the cell culture media were collected by precipitation with ammonium sulfate and purified by ultracentrifugation on an iodixanol gradient. The particles were then concentrated by exchanging iodixanol for Lactate Ringer's solution by multiple dilution and concentration steps using a centrifugal concentrator. The AAV titer was determined by quantitative real-time PCR and SDS-PAGE. AAV9-GFP was used as control.

  Result-1

  1. AAV viral vector with Troponin T promoter shows better yield than Periostin promoter in terms of viral production presumably due to higher promoter activity (Figure 2, upper panel)
  2. Alkaline gel staining results show that the purified AAV vectors do not show any genomic degradataion (Firgure 2, middle panel)
  3. EM picture (Figure 2, lower panel) reveals that more than 70% viral particle are fully packed with DNA, which indicates that the purified viral vectors are functional.

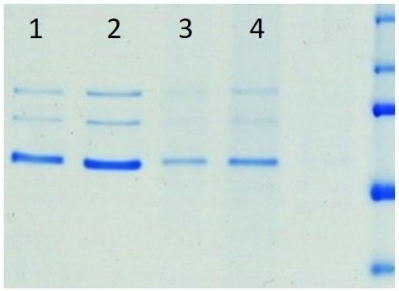

Coomassie blue staining

1. AAV9 Enh-TnT-miR TuD (2ul)
2. AAV9 Enh-TnT-miR TuD(4ul)
3. AAV9 Enh-Postn-miR TuD (2ul)
4. AAV9 Enh-Postn-miR TuD (4ul)

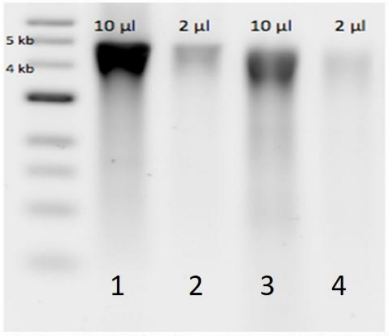

Alkaline gel staining

1. AAV9 Enh-TnT-miR TuD (10ul)
2. AAV9 Enh-TnT-miR TuD(2ul)
3. AAV9 Enh-Postn-miR TuD (10ul)
4. AAV9 Enh-Postn-miR TuD (2ul)

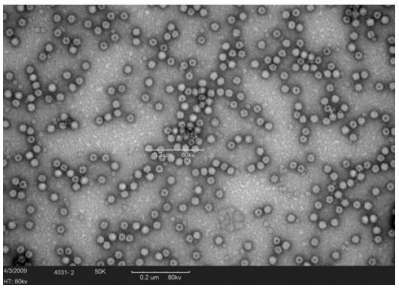

EM picture

AAV9 Enh-TnT-miR TuD

Figure 2. AAV9 Enh-TnT/ Enh-Postn-miR-25 TuD production and quality control.
Upper panel: Coomassie blue staining result for AAV9 Enh-TnT / Enh-Postn miR-25 TuD.
Middle panel: Alkaline gel staining result for AAV9 Enh-TnT / Enh-Postn miR-25 TuD.
Lower panel: Electron Microscopy picture with negative staining for AAV9 Enh-TnT miR-25 TuD.

Result-2

1. AAV9 vectors with four different promoters (1e5 vg / cell) were transfected into the primary adult isolated cardiomyocytes (CMs). 5 days later, each transfected CM was harvested and miR-25 expression levels were measured. As shown in Figure 3, CMV promoter shows the most efficient inhibition of miR-25 expression and U6 and Enh-TnT promoters show comparable activity, which inhibit 50% reduction in miR-25 expression. On the other hand, Enh-Postn promoter didn't show any inhibitory effect on miR-25 expression in CMs, which indicates that Postn promoter doesn't have transduction activity on CMs.

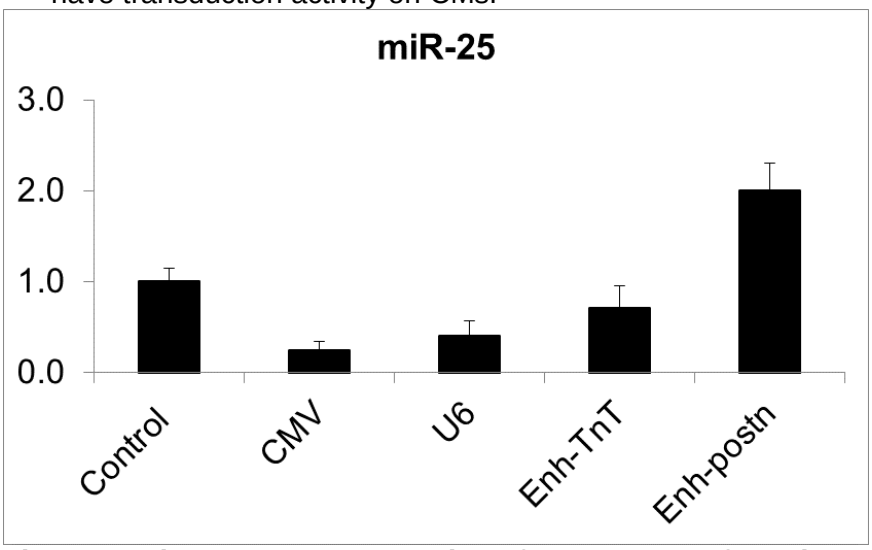

Figure 3. miR-25 mRNA expression after gene transfer using various promoters-derived AAV vectors.

Subtask 4: Evaluation of cis-regulatory module (Enhancer) with Periostin (Postn) promoter in myofibroblasts specificity.

- Experiments and analysis were completed on Aug, 2020.

Method

Isolation of primary cardiaomyocytes (CMs) and cardiac fibroblasts (CFBs)

To isolate in tissue primary cardiac cells from the heart tissue, Langendorff-based isolation was applied as utilizing previous protocol [33]. In brief, after heparin (50 U) was injected, animals were anaesthetized with intra-peritoneal ketamine (100mg/g). The heart was quickly removed from the chest and the aorta was retrogradely perfused at 37 °C for 3 min with calcium-free Tyrode buffer (137 mM NaCl, 5.4 mM KCl, 1 mM MgCl2, 10 mM glucose, 10 mM HEPES [pH 7.4], 10 mM 2, 3-butanedione monoxime, and 5 mM taurine) gassed with 100% O2. The enzymatic digestion was initiated by adding collagenase type B (300 U/ml; Worthington) and hyaluronidase (0.1 mg/ml; Worthington) to the perfusion solution. When the heart became swollen after 10 min of digestion, the left ventricle was quickly removed, cut into several chunks, and further digested in a shaker (60-70 rpm) for 10 min at 37°C in the same enzyme solution. The cell suspension was filtered through a cell strainer (100 µm pore size; BD Falcon) and gently centrifuged at 500 rpm for 1 min. This procedure usually yielded ≥ 80% viable rod-shaped ventricular myocytes with clear sarcomere striations. The isolated cardiomyocytes were plated onto a laminin-coated plate and cultured in modified Eagle′s Medium (MEM) with Hanks′ Balanced Salt solution, supplemented with 2 mM of L-carnitine, 5 mM of creatine and 5 mM of taurine, and 100 IU/ml of penicillin.

Results

1. AAV9 Enh-Postn miR-25 TuD efficiently reduces miR-25 expression as comparable as CMV promoter.
2. AAV9 Enh-TnT miR-25 TuD failed to inhibit miR-25 expression in primary CFBs.

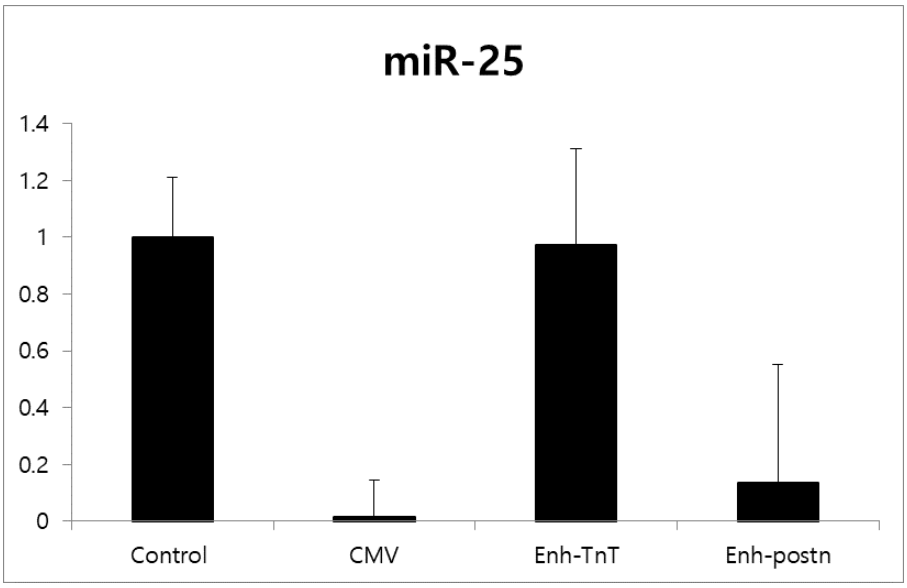

Figure 4. AAV9 Enh-postn miR-25 TuD exclusively down-regulates miR-25 expression in primary cardiac fibroblasts (CFBs) but not Enh-TnT.

Subtask 5: Characterize the biodistribution for miR-25 expression.

- Experiments and analysis are ongoing.
- Mice were injected with AAV9 vectors and all planned experiments will be completed by Nov, 2020.

Methods

Quantitative real-time PCR

Transcript levels were determined by real-time PCR using a QuantiTect SYBR Green real time PCR Kit (Qiagen Ltd; Valencia CA). Total RNA was isolated from samples with Trizol reagent (Gibco BRL; Carlsbad, CA) according to the manufacturer's instructions. Reverse transcription was performed at 50°C for 20 min, and cDNA was amplified in 20 µL reaction volumes using 10pmol of primers for 37 cycles: 94°C for 10 s, 57°C for 15 s, and 72°C for 5 s. 18S RNA was used as an internal control to calculate the relative abundance of the mRNAs.

Western blot analysis

Membrane and tissue homogenates were prepared as previously described (Wahlquist et al., 2014). Proteins were resolved on 10% SDS-PAGE gels followed by transfer to PVDF membranes (Millipore, MA, USA). Detection of the proteins bands was performed according to standard lab protocols. Antibody raised against SERCA2a was produced by 21st Century Biochemicals, and were purchased from Lifespan biosciences (Seattle, USA) and antibody raised against Smad7 (B-8) from Santa Cruz Biotechnology (CA, USA).

Results

Total 40 mice were injected with each AAV with different promoters (10 mice each) on Aug 13th, 2020. Mice will be sacrificed in six weeks.

Subtask 6: Comparison between ubiquitous CMV promoter with newly generated tissue specific promoters.

- Experiments and analysis are ongoing.
- In Figure 2, I have already shown the comparison result using primary isolated cardiomyocytes and fibroblasts in vitro but in vivo experiments have not been accomplished.

Method

Mice are monitored daily basis and recorded.

Echocardiograpghy and Treadmill (exhaustion test) will be applied to each group of mice and analyzed.

Results

Cardiac and skeletal functions will be evaluated six weeks after gene transfer.

3) What opportunities for training and professional development has the project provided?

1) Junior Faculty Mentorship Committee Meeting was held in Feb, 2020.
2) Rigor and Reproducibility and Ethical Behavior in Biomedical Research course was completed July 31st, 2020.

4) How were the results disseminated to communities of interest?

HF is characterized by a debilitating decline in cardiac function, in which calcium dysregulation occurs. Of the many intracellular mechanisms that contribute to Ca^{2+} handling, the sarcoplasmic endoplasmic reticulum ATPase 2a (SERCA2a) has been shown to be the dominant generator of Ca^{2+} re-uptake within cardiomyocytes during cardiac relaxation. Furthermore, it has previously been shown that both SERCA2a mRNA and protein expression are significantly decreased in the hearts of MDX mice. Subsequently, increased SERCA2a expression via gene transfer has been shown by our group to improve ECG performance in aged MDX mice. Recently, we have found that miR-25 is a key microRNA that regulates SERCA2a and we showed anti-miR25 treatment enhanced cardiac contractility and function through SERCA2a restoration in murine HF models. From this result, we hypothesize that inhibition of miR-25 expression may be one of promising therapeutic approach to enhance cardiac function in DMD-induced cardiomyopathy. However, the expression of cardiac miR-25 in the preclinical DMD animal models or DMD patients has not been elucidated. Therefore, we evaluated the expression of miR-25 in DMD mouse model. As a result, we found that miR-25 expression is significantly increased and SERCA2a and SMAD7 expression are down-regulated in DMD. Since we have identified Smad7 as a new target of miR-25, miR-25 TuD treatment maybe suggested as a dual-therapeutic intervention to normalize cardiac function and fibrosis, respectively in DMD patient.

5) What do you plan to do during the next reporting period to accomplish the goals?

Modified SOW for No-cost extension for the rest of funding period;

Specific Aim 2: Therapeutic evaluation of miR-25 TuD using cell type specific promoters		
Major Task 2: Development of cell type specific promoter with miR-25 TuD in an AAV9 vector	**Months**	**Achievements**
Subtask 1: Develop of AAV construct containing Troponin T (TnT) promoter with cis-elementary module (aka enhancer (Enh)) for cardiomyocyte specific expression of miR-25 TuD	14-15	**Completed**
Subtask 2: Develop of AAV construct containing Periostin (Postn) promoter with cis-elementary module (aka enhancer (Enh)) for cardiac myofibroblast specific expression of miR-25 TuD	15-17	**Completed**
Subtask 3: Evaluation of cis-regulatory module with TnT promoter in cardiomyocyte specificity (20 mice per group x 2 groups = 40 mice total)	24-26	**Ongoing**
Subtask 4: Evaluation of cis-regulatory module with Periostin (Postn) promoter in myofibroblasts specificity (20 mice per group x 2 groups = 40 mice total)	24-26	**Ongoing**
Subtask 5: Characterize the biodistribution for miR-25 expression	26-27	**Ongoing**

(20 mice per group x 2 groups = 40 mice total)		
Subtask 6: Comparison between ubiquitous CMV promoter with newly generated tissue specific promoters (20 mice per group x 2 groups = 40 mice total)	26-27	**Ongoing**
Milestone(s) Achieved: Characterization of effects of cell type specific promoter with enhancer in terms of miR-25 expression and cardiac function	30	

Due to the COVID-19 outbreak in New York, which is my primary performance site, many critical experiments for my award have been heavily restricted so that my entire research has been delayed. Therefore, I requested a No-cost extension on June 9th, 2020 and obtained an approval letter on June 22nd. The new project end date is February 14th, 2021.

4. IMPACT:

1) What was the impact on the development of the principal discipline(s) of the project?

- **Normalization of miRNA levels as a therapeutic approach for DMD-induced cardiomyopathy.** Cardiac gene therapy is emerging as a novel strategy to treat inherited and acquired cardiomyopathies. miRNAs are interesting targets for gene transfer because individual miRNA regulates collections of mRNA expression that often have related functions, thereby governing complex biological processes. Therefore, deregulation of one particular miRNA is sometimes enough to cause a specific cardiac disease, while small effects of miRNA can be amplified and generate striking alterations. However, there are many hurdles to overcome before miRNA gene transfer can be used for treating cardiac diseases clinically. Challenges include, but are not limited to, cardiac targeting, optimal dosing, appropriate vector, and choice of targeting the right miRNAs. Currently, there is no report of viral vector mediated miRNA gene transfer for treating DMD-induced cardiomyopathy in large animals or clinical studies. We have developed a cardiac specific promoter consisting of a TnT promoter with a calsequestrin enhancer that restricts expression to the cardiac cells while de-targeting the liver and lungs. Our group has extensive experience in using AAV vectors for treating HF, with successful results also in large animal studies. Taking advantage of our expertise, we aim to establish a viral-mediated decoy down regulation of miR-25 approach in a DMD-induced cardiomyopathy model.

2) What was the impact on other disciplines?

- **Application for government sponsored research grant**
  We have demonstrated that small non-coding microRNA can be a therapeutic target to treat DMD-induced cardiomyopathy from this research. Therefore, a reasonable next step is to apply a government sponsored grant to continue further validation of our finding in the setting of large animal model for translational research.

3) What was the impact on technology transfer?

Nothing to report

4) What was the impact on society beyond science and technology?

- Heart disease profoundly affects the quality of life of Duchenne Muscular Dystrophy (DMD) patients. Over a couple of decades, many approaches have been made clinically to treat DMD but no cure has been reported yet. Therefore, novel therapeutic approach for DMD is highly demanding. miR-25 has been known a major regulator for SERCA2a, a critical calcium regulator in cardiac function. Furthermore, we have observed that this particular miRNA is upregulated in DMD-induced cardiomyopathy models. Therefore, it is critical to understand the underlying mechanism of miR-25 for the treatment of DMD patient with cardiac abnormality.

5. CHANGES/PROBLEMS:

I have requested the No-cost extension (NCE) for this particular grant due to COVID-19 pandemic. As a result, the NCE application was approved on June 22nd, 2020. Therefore, the new project end date was changed to Feb 14th, 2021

6. PRODUCTS:

1) Publications, conference papers, and presentations;

- **Published articles**

a. Oh JG, Lee P, Gordon RE, Sahoo S, Kho C, **Jeong D****. Analysis of extracellular vesicle miRNA profiles in heart failure. ***J Cell Mol Med. 2020 Jun 2;24(13):7214-7227. doi: 10.1111/jcmm.15251.***

b. Lee MA, Raad N, Song MH, Yoo J, Lee M, Jang SP, Kwak TH, Kook H, Choi E, Cha T, Hajjar RJ, **Jeong D****, Park WJ**. The matricellular protein CCN5 prevents adverse atrial structural and electrical remodeling. ***J Cell Mol Med. 2020 July 30 (in press)***

- **Pending articles**

a. Sacha V. Kepreotis, MBBS*; Min Ho Song, BS*; Jimeen Yoo, MS; Jae Gyun Oh, PhD; Changwon Kho, PhD; Brian Brown, PhD; Agustin Rojas-Muñoz, PhD; Christine Wahlquist, PhD; Mark Mercola, PhD; Fadi Akar, PhD; Dongtak Jeong, PhD**. AAV9 miR-25 tough decoy transfer improves cardiac function in aged MDX/UTRN KO mice. ***Under revision***

.

- **Presentations**

a. MDA conference 2020, Orlando, FL (On-line)
Title: miR-25 Tough Decoy enhances cardiac contractility and ameliorates cardiac fibrosis in aged MDX/UTRN KO Mice.

2) licenses applied for and/or issued;
Nothing to Report

3) degrees obtained that are supported by this training grant;
Nothing to Report

4) development of cell lines, tissue or serum repositories;
Nothing to Report

5) informatics such as databases and animal models, etc.;
Nothing to Report

6) funding applied for based on work supported by this training grant;

I. NIH/NHLBI 04/01/2021 - 03/31/2025
Title: The therapeutic potential of CCN5 in myocardial fibrosis associated with heart failure
Role: Principal Investigator

II. NIH/NHLBI 04/01/2020 - 03/31/2025
Title: Targeting RV fibrosis in chronic pulmonary hypertension
Role: Co-Investigator

III. Department of Defense-Development Award (DA) 03/01/2021- 2/28/2023
Title: Inhibition of miR-25 attenuates pulmonary arterial hypertension associated with congenital heart defects
Role: Principal Investigator

7. PARTICIPANTS & OTHER COLLABORATING ORGANIZATIONS

What individuals have worked on the project?
Nothing to Report

Has there been a change in the active other support of the PD/PI(s) or senior/key personnel since the last reporting period?
Nothing to Report

What other organizations were involved as partners?
Nothing to Report

8. SPECIAL REPORTING REQUIREMENTS

1) **COLLABORATIVE AWARDS:**
   Nothing to Report

2) **AWARD CHARTS:**
   Attached in Appendix section

9. REFERENCES

1 Cox, G. F. & Kunkel, L. M. Dystrophies and heart disease. *Curr Opin Cardiol* **12**, 329-343 (1997).

2 Duan, D. Challenges and opportunities in dystrophin-deficient cardiomyopathy gene therapy. *Hum Mol Genet* **15 Spec No 2**, R253-261, doi:10.1093/hmg/ddl180 (2006).

3 Bostick, B., Yue, Y., Long, C. & Duan, D. Prevention of dystrophin-deficient cardiomyopathy in twenty-one-month-old carrier mice by mosaic dystrophin expression or complementary dystrophin/utrophin expression. *Circ Res* **102**, 121-130, doi:10.1161/CIRCRESAHA.107.162982 (2008).

4 Inkley, S. R., Oldenburg, F. C. & Vignos, P. J., Jr. Pulmonary function in Duchenne muscular dystrophy related to stage of disease. *Am J Med* **56**, 297-306 (1974).

5 Ishizaki, M. *et al.* Mdx respiratory impairment following fibrosis of the diaphragm. *Neuromuscul Disord* **18**, 342-348, doi:10.1016/j.nmd.2008.02.002 (2008).

6 Mukoyama, M., Hizawa, K., Kagawa, N. & Takahashi, K. [The life spans, cause of death and pathological findings of Fukuyama type congenital muscular dystrophy--analysis of 24 autopsy cases]. *Rinsho Shinkeigaku* **33**, 1154-1156 (1993).

7 Wehling-Henricks, M. *et al.* Arginine metabolism by macrophages promotes cardiac and muscle fibrosis in mdx muscular dystrophy. *PLoS One* **5**, e10763, doi:10.1371/journal.pone.0010763 (2010).

8 Baxter, P. Treatment of the heart in Duchenne muscular dystrophy. *Dev Med Child Neurol* **48**, 163, doi:10.1017/S0012162206000351 (2006).

9 Finsterer, J. & Stollberger, C. The heart in human dystrophinopathies. *Cardiology* **99**, 1-19, doi:68446 (2003).

10 Miyoshi, K. Echocardiographic evaluation of fibrous replacement in the myocardium of patients with Duchenne muscular dystrophy. *Br Heart J* **66**, 452-455 (1991).

11 Kubo, M., Matsuoka, S., Taguchi, Y., Akita, H. & Kuroda, Y. Clinical significance of late potential in patients with Duchenne muscular dystrophy. *Pediatr Cardiol* **14**, 214-219, doi:10.1007/BF00795373 (1993).

12 Yanagisawa, A. *et al.* The prevalence and prognostic significance of arrhythmias in Duchenne type muscular dystrophy. *Am Heart J* **124**, 1244-1250 (1992).

13 Alloatti, G., Gallo, M. P., Penna, C. & Levi, R. C. Properties of cardiac cells from dystrophic mouse. *J Mol Cell Cardiol* **27**, 1775-1779 (1995).

14 Dunn, J. F. & Radda, G. K. Total ion content of skeletal and cardiac muscle in the mdx mouse dystrophy: Ca2+ is elevated at all ages. *J Neurol Sci* **103**, 226-231 (1991).

15 Fauconnier, J. *et al.* Leaky RyR2 trigger ventricular arrhythmias in Duchenne muscular dystrophy. *Proc Natl Acad Sci U S A* **107**, 1559-1564, doi:10.1073/pnas.0908540107 (2010).

16 Goonasekera, S. A. *et al.* Mitigation of muscular dystrophy in mice by SERCA overexpression in skeletal muscle. *J Clin Invest* **121**, 1044-1052, doi:10.1172/JCI43844 (2011).

17 Williams, I. A. & Allen, D. G. Intracellular calcium handling in ventricular myocytes from mdx mice. *Am J Physiol Heart Circ Physiol* **292**, H846-855, doi:10.1152/ajpheart.00688.2006 (2007).

18 Sarma, S. *et al.* Genetic inhibition of PKA phosphorylation of RyR2 prevents dystrophic cardiomyopathy. *Proc Natl Acad Sci U S A* **107**, 13165-13170, doi:10.1073/pnas.1004509107 (2010).

19 Kawase, Y. & Hajjar, R. J. The cardiac sarcoplasmic/endoplasmic reticulum calcium ATPase: a potent target for cardiovascular diseases. *Nat Clin Pract Cardiovasc Med* **5**, 554-565, doi:10.1038/ncpcardio1301 (2008).

20 Lipskaia, L., Chemaly, E. R., Hadri, L., Lompre, A. M. & Hajjar, R. J. Sarcoplasmic reticulum Ca(2+) ATPase as a therapeutic target for heart failure. *Expert Opin Biol Ther* **10**, 29-41, doi:10.1517/14712590903321462 (2010).

21 Shin, J. H., Bostick, B., Yue, Y. P., Hajjar, R. & Duan, D. S. SERCA2a gene transfer improves electrocardiographic performance in aged mdx mice. *J Transl Med* **9**, doi:Artn 13210.1186/1479-5876-9-132 (2011).

22 Brown, B. D. & Naldini, L. Exploiting and antagonizing microRNA regulation for therapeutic and experimental applications. *Nat Rev Genet* **10**, 578-585, doi:10.1038/nrg2628 (2009).

23 Condorelli, G., Latronico, M. V. & Cavarretta, E. microRNAs in cardiovascular diseases: current knowledge and the road ahead. *J Am Coll Cardiol* **63**, 2177-2187, doi:10.1016/j.jacc.2014.01.050 (2014).

24 Melman, Y. F., Shah, R. & Das, S. MicroRNAs in heart failure: is the picture becoming less miRky? *Circ Heart Fail* **7**, 203-214, doi:10.1161/CIRCHEARTFAILURE.113.000266 (2014).

25 Mullokandov, G. *et al.* High-throughput assessment of microRNA activity and function using microRNA sensor and decoy libraries. *Nat Methods* **9**, 840-846, doi:10.1038/nmeth.2078 (2012).

26 Wahlquist, C. *et al.* Inhibition of miR-25 improves cardiac contractility in the failing heart. *Nature* **508**, 531-535, doi:10.1038/nature13073 (2014).

27 Bish, L. T. *et al.* Adeno-associated virus (AAV) serotype 9 provides global cardiac gene transfer superior to AAV1, AAV6, AAV7, and AAV8 in the mouse and rat. *Hum Gene Ther* **19**, 1359-1368, doi:10.1089/hum.2008.123 (2008).

28 Fechner, H. *et al.* Expression of coxsackie adenovirus receptor and alphav-integrin does not correlate with adenovector targeting in vivo indicating anatomical vector barriers. *Gene Ther* **6**, 1520-1535, doi:10.1038/sj.gt.3301030 (1999).

29 Hiltunen, M. O. *et al.* Biodistribution of adenoviral vector to nontarget tissues after local in vivo gene transfer to arterial wall using intravascular and periadventitial gene delivery methods. *FASEB J* **14**, 2230-2236, doi:10.1096/fj.00-0145com (2000).

30 Rincon, M. Y. *et al.* Genome-wide computational analysis reveals cardiomyocyte-specific transcriptional Cis-regulatory motifs that enable efficient cardiac gene therapy. *Mol Ther* **23**, 43-52, doi:10.1038/mt.2014.178 (2015).

31 Kanisicak, O. *et al.* Genetic lineage tracing defines myofibroblast origin and function in the injured heart. *Nat Commun* **7**, 12260, doi:10.1038/ncomms12260 (2016).

32 Iannello, R. C., Mar, J. H. & Ordahl, C. P. Characterization of a promoter element required for transcription in myocardial cells. *J Biol Chem* **266**, 3309-3316 (1991).

33 Oh, J.G. *et al.* PICOT increases cardiac contractility by inhibiting PKCzeta activity. *Journal of molecular and cellular cardiology* 53, 53-63 (2012).

34 Zolotukhin, S. *et al.*, Byrne, B.J., Mason, E., Zolotukhin, I., Potter, M., Chesnut, K., Summerford, C., Samulski, R.J., and Muzyczka, N.. Recombinant adeno-associated virus purification using novel methods improves infectious titer and yield. *Gene therapy* 6, 973-985 (1999).

10. APPENDICES:

1) Modified contract notice with No-cost extension (NCE)

Impact:

This FY17 DMDRP Focus Area is cardiac studies, proposing to apply potential therapeutic interventions for DMD caused cardiac dysfunction and fibrosis. Ultimately, this research will help older DMD patients, a growing subpopulation due to improved respiratory care, who is suffering from cardiac dysfunction and fibrosis that affect patient's quality of life. Clinically, there is potential for gene therapy by inhibiting a miR-25 using tissue specific viral vectors and transcription factors to improve cardiac regulation. Furthermore, by using a single microRNA to improve both cardiac contractility and decrease potential fibrosis, symptoms due to cardiac issues will be decreased.

ii. Funding Overview

	Federal funds	Cost Sharing	Total amount
a. Obligated or deobligated this action	$0	N/A	$0
b. Cumulative obligations to date, including this and previous actions	$464,180.00	N/A	$464,180.00
c. Planned project costs in the currently approved budget through the end of the period of performance, to include any future incremental funding obligations	$464,180.00	N/A	$464,180.00
d. Total value, which includes any unexercised options for which amounts were established in the award	$464,180.00	N/A	$464,180.00

6. **Obligation/Effective Date:** See SF-30, Block 16c.
7. **Period of performance:** 15 August 2018 – 14 February 2021
8. **Authorities:** This award is made under the authority of 10 U.S.C. 2358.
9. **Catalog of Federal Domestic Assistance Number:** 12.420-Military Medical Research and Development
10. **Project Performance Information:**
    - i. This award is for research and development. Construction activities under this award are not authorized. (Reference Department of the Army Pamphlet 420-11, dated 18 March 2010, for the definition of construction activities.)
    - ii. Statement of Work and Budget: The revised Statement of Work (SOW) dated 20 June 2018 and the revised budget dated 20 June 2018 for your application submitted in response to the Fiscal Year 2017 DoD Duchenne Muscular Dystrophy Research Program, Career Development Award, Program Announcement (Funding Opportunity Announcement Number W81XWH-17-DMDRP-CDA, which closed 10/18/2017) are incorporated herein by reference. You may rebudget allowable costs in accordance with applicable cost principles and in accordance with the prior approval requirements as stated in this award. Additional terms and conditions applicable to this award are in Division II and Division III.
    - iii. The following terms and conditions are incorporated herein by reference:
        - a. Division III - USAMRAA Addendum to the DoD R&D General Terms and Conditions available at http://www.usamraa.army.mil/Pages/Resources.aspx.
        - b. The DoD R&D General Terms and Conditions (September 2017), available at http://www.onr.navy.mil/Contracts-Grants/submit-proposal/grants-proposal/grants-terms-conditions.aspx.
    - iv. These USAMRAA Award Specific Research Terms and Conditions are in addition to the terms and conditions incorporated above. Any inconsistencies in the requirements of this award will be resolved in the following order:
        - a. Federal statutes
        - b. Federal regulations

2) Award chart

W81XWH-18-1-0322 (Annual Phase II): Targeting Cardiac Calcium Regulation and Fibrosis in DMD Models

PI: Dongtak Jeong, PhD, Icahn School of Medicine at Mount Sinai, NY

Budget: $ 464,180.00 **Topic Area:** DMDRP **Mechanism:** FY17-DMDRP-CDA

Research Area(s): 0810 (Gene therapy) **Award Status:** 15 August 2018 – 14 February 2021

Study Goals: Since miR-25 has been found to affect both cardiac function and fibrosis, it is hypothesized that therapeutic application of AAV9 miR-25 Tough Decoy (TuD) will rescue the cardiac dysfunction and fibrosis phenotypes of DMD.

Specific Aims:

Aim 1: Therapeutic evaluation of miR-25 TuD on cardiac function and fibrosis.
Aim 2: Therapeutic evaluation of miR-25 TuD using cell type specific promoters.

Key Accomplishments and Outcomes:

Publications:

- **Published articles**

a. Oh JG, Lee P, Gordon RE, Sahoo S, Kho C, **Jeong D****. Analysis of extracellular vesicle miRNA profiles in heart failure. ***J Cell Mol Med. 2020 Jun 2;24(13):7214-7227. doi: 10.1111/jcmm.15251.***

b. Lee MA, Raad N, Song MH, Yoo J, Lee M, Jang SP, Kwak TH, Kook H, Choi E, Cha T, Hajjar RJ, **Jeong D****, Park WJ**. The matricellular protein CCN5 prevents adverse atrial structural and electrical remodeling. ***J Cell Mol Med. 2020 July 30 (in press)***

- **Pending articles**

a. Sacha V. Kepreotis, MBBS*; Min Ho Song, BS*; Jimeen Yoo, MS; Jae Gyun Oh, PhD; Changwon Kho, PhD; Brian Brown, PhD; Agustin Rojas-Muñoz, PhD; Christine Wahlquist, PhD; Mark Mercola, PhD; Fadi Akar, PhD; Dongtak Jeong, PhD**. AAV9 miR-25 tough decoy transfer improves cardiac function in aged MDX/UTRN KO mice. ***Under revision***

Patents: none to date

Funding Obtained: pending

- NIH/NHLBI 04/01/2021 - 03/31/2025
  Title: The therapeutic potential of CCN5 in myocardial fibrosis associated with heart failure, Role: Principal Investigator
- NIH/NHLBI 04/01/2020 - 03/31/2025
  Title: Targeting RV fibrosis in chronic pulmonary hypertension, Role: Co-Investigator
- Department of Defense-Development Award (DA) 03/01/2021- 2/28/2023
  Title: Inhibition of miR-25 attenuates pulmonary arterial hypertension associated with congenital heart defects
  Role: Principal Investigator

3) **Original copy for the publications**

I. Oh JG, Lee P, Gordon RE, Sahoo S, Kho C, **Jeong D****. Analysis of extracellular vesicle miRNA profiles in heart failure. ***J Cell Mol Med. 2020 Jun 2;24(13):7214-7227. doi: 10.1111/jcmm.15251.***

Received: 4 December 2019 | Revised: 25 February 2020 | Accepted: 13 March 2020

DOI: 10.1111/jcmm.15251

ORIGINAL ARTICLE

WILEY

Analysis of extracellular vesicle miRNA profiles in heart failure

Jae Gyun Oh[1] | Philyoung Lee[1] | Ronald E. Gordon[2] | Susmita Sahoo[1] | Changwon Kho[1,3] | Dongtak Jeong[1]

[1]Cardiovascular Research Center, Icahn School of Medicine at Mount Sinai, New York, NY, USA

[2]Pathology Department, Icahn School of Medicine at Mount Sinai, New York, NY, USA

[3]Division of Applied Medicine, School of Korean Medicine, Pusan National University, Republic of Korea

Correspondence
Dongtak Jeong, PhD, Cardiovascular Research Center, Icahn School of Medicine at Mount Sinai (ISMMS), 1 Gustave L. Levy place, New York, NY, USA.
Email: dongtak.jeong@mssm.edu

Funding information
Congressionally Directed Medical Research Programs, Grant/Award Number: W81XWH-18-1-0322 and W81XWH-19-1-0382; American Heart Association, Grant/Award Number: 18TPA34170460

Abstract

Extracellular vesicles (EVs) have recently emerged as an important carrier for various genetic materials including microRNAs (miRs). Growing evidences suggested that several miRs transported by EVs were particularly involved in modulating cardiac function. However, it has remained unclear what miRs are enriched in EVs and play an important role in the pathological condition. Therefore, we established the miR expression profiles in EVs from murine normal and failing hearts and consecutively identified substantially altered miRs. In addition, we have performed bioinformatics approach to predict potential cardiac outcomes through the identification of miR targets. Conclusively, we observed approximately 63% of predicted targets were validated with previous reports. Notably, the predicted targets by this approach were often involved in both beneficial and malicious signalling pathways, which may reflect heterogeneous cellular origins of EVs in tissues. Lastly, there has been an active debate on U6 whether it is a proper control. Through further analysis of EV miR profiles, miR-676 was identified as a superior reference control due to its consistent and abundant expressions. In summary, our results contribute to identifying specific EV miRs for the potential therapeutic targets in heart failure and suggest that miR-676 as a new reference control for the EV miR studies.

KEYWORDS

bioinformatics, extracellular vesicle, heart failure, microRNA, microRNA array, microRNA control, miR-676, U6

1 | INTRODUCTION

A heart is a highly complex structure composed of multiple types of cellular and acellular tissues.[1,2] Of cardiac components, cardiomyocyte is a major contributor to cardiac composition and output.[1] Non-myocytes such as fibroblasts, leucocytes and endothelial cells serve as a spatial buffer and more importantly modulate cardiomyocyte functions in response to physiological and pathological stimuli. Thus, cardiomyocytes and non-myocytes closely communicate to maintain cardiac homeostasis, and the imbalance in this communication causes cardiac diseases.[3] Metabolites such as nitric oxide and reactive oxygen species and signalling molecules including extracellular matrix proteins, cytokines and growth factors are known to be classic mediators of intercellular communication.[3,4]

Recently, extracellular vesicles (EVs) emerged as a mechanism underlying this intercellular communication. Although EVs had incipiently been considered as a means of cellular waste disposal, accumulating data recently indicated that genetic cargos such as mRNAs,

[†]Oh and Lee contributed equally to this manuscript.

microRNAs (miRs) and proteins are transported by EVs. Therefore, EVs are being re-evaluated as a critical modifier of cellular functions.[5] During last decade, tremendous efforts have been placed to understand the mechanism and the function of EVs in diverse fields of studies including cardiovascular researches. For example, EVs derived from stem cells or cardiac progenitor cells were generally beneficial,[6–9] whereas EVs from fibroblasts or endothelial cells exhibited deleterious effects on cardiac functions.[10–12] In these previous studies, the origin of EVs was confined to in vitro cultured cells or blood plasma, but the role of EVs in cardiac tissues has been poorly investigated. Therefore, it is important to characterize in tissue EVs under pathological conditions. Recently, Loyer X. et al characterized the functions of EVs isolated from mouse hearts subjected to myocardial infarction.[13] In this study, we further analysed the expression profiles and functions of miRNAs in EVs isolated from pressure overload-induced failing hearts compared to normal hearts.

Apart from the characterization study, we also sought to identify an alternative internal reference for miR studies. In general, U6 is the most commonly used control for the normalization of miR expression. However, it is yet controversial whether U6 is a suitable control because variable expression patterns of U6 were observed in a number of studies.[14–19] Analysing the abundancy and stability of miR expression, U6 was confirmed as an appropriate control being consistently expressed throughout our samples. In addition, we identified miR-676 as an alternative candidate as a control and observed that it exhibited a significant correlation with U6. Taken together, although a further validation is necessary in other tissues or organs, miR-676 may serve as an alternative control for the EV miR studies in the heart.

In summary, this study analysed miR profiles in the cardiac EVs isolated from murine normal and failing hearts. Our results demonstrated that the cardiac EVs contain diverse miRs with contradictory functions. The results may reflect various cellular origins of EVs and dynamic alternations of miR expressions in these EVs during heart failure. Nevertheless, our study may contribute to understand intercellular communication between cardiac cells under the pathological condition and suggests EV miRs as potential biomarkers and therapeutic targets for the intervention of heart failure.

2 | MATERIALS AND METHODS

2.1 | Animal care and TAC

All procedures were approved by and performed in accordance with the Institutional Animal Care and Use Committee of the Mount Sinai School of Medicine. The investigation conformed to the Guide for the Care and Use of Laboratory Animals published by the US National Institutes of Health (NIH Publication No. 85-23, revised 1996). Studies were conducted in male C57BL/6 mice aged 8 – 10 weeks (weight, 25 – 30 g) obtained from Jackson Laboratories. Transverse aortic constriction (TAC) was conducted as previously described with minor modifications.[10] Briefly, mice were anesthetized with a solution mixture of 95 mg/kg ketamine and 5 mg/kg xylazine administered via intraperitoneal injection. The transverse aortic arch was ligated between the innominate and left common carotid arteries with an overlaid 27-gauge needle. The needle was then immediately removed, leaving a discrete region of constriction. Two month after TAC operation, the mice showed less than 40% of fractional shortening in average which is typically considered as failing heart and included in this study (Figure S3). Sham-operated mice underwent the same surgical procedures, except that the ligature was not tied.

2.2 | EV isolation and purification

To isolate in tissue cardiac EVs from the heart tissue, Langendorff-based isolation was applied as utilizing previous protocol to isolate in tissue EV from liver.[20] Hearts were extracted from sham or TAC-operated animals, and the aorta was retrogradely perfused at 37°C for 3 minutes with Tyrode buffer (137 mmol/L NaCl, 5.4 mmol/L KCl, 1 mmol/L $MgCl_2$, 10 mmol/L glucose, 10 mmol/L HEPES [pH 7.4], 10 mmol/L 2, 3-butanedione monoxime, and 5 mmol/L taurine) gassed with 100% O_2. The enzymatic digestion was initiated by the addition of collagenase type B (300 U/mL; Worthington) and hyaluronidase (0.1 mg/mL; Worthington) to the perfusion solution. After 20 minutes of digestion, the heart tissue was removed, cut into several chunks and gently pipetted for 2 minutes in Tyrode buffer with 5% BSA. The mixtures of cell, extracellular matrix and EVs were then separated by several centrifugations according to a previously described protocol.[21] EVs were pelleted by ultracentrifugation at 100 000 × *g* at 4°C for 90 minutes and resuspended in 200 μL of PBS solution.

2.3 | Transmission Electron microscopy for EVs with negative staining

EVs from fresh ventricles were collected as described above and pre-fixed with 2% paraformaldehyde (PFA) for 30 minutes. Deposit 5 μL resuspended pellets on Formvar-carbon-coated EM grid. Add 10 μL of 2% uranyl acetate on the grid and incubate for another 10 minutes. After thorough washes, store grid in the grid box at room temperature and dark until imaging. Samples were viewed under a transmission electron microscope (HITACHI H-7650, Japan) operated at 80 kV. Images were taken at 10K, 20K and 30K-folds magnification.

2.4 | Western blot of EV markers and Coomassie blue stain

50 μL of EV samples from Sham and TAC EV was directly mixed with 5x SDS sample buffer, boiled at 95°C for 3 minutes and then separated on a SDS-PAGE gel. The total loaded protein amount was calculated by the intensity of Coomassie blue stain. The membrane

was blocked in 5% skim milk solution and incubated overnight with an antibody directed against hnRNA A2B1 (Ab6102, Abcam, 1:5000), CD63 (Ab1318, Abcam, 1:1000), Flotillin 1 (Ab133497, Abcam, 1:10 000), TSG101 (Ab83, Abcam, 1:1000), H3 (Ab1791, Abcam, 1:1000) and SERCA2a (custom antibody from 21st Century Biochemicals, 1:3000). The membrane was then incubated with a horseradish peroxidase-conjugated secondary antibody (Sigma) and developed with Western Lighting chemiluminescence reagent (PerkinElmer).

2.5 | Nanoparticle tracking analysis

Samples were loaded into the assembled sample chamber of a NanoSight LM10. 60-second video images were acquired by a Hamamatsu C11440 ORCA-Flash 2.8 digital camera and analysed by NanoSight NTA 2.3 software.

2.6 | Extracellular vesicle microRNA isolation and microRNA array profiling

100 μL of EV samples from Sham and TAC EV was used to extract RNA for microRNA array profiling and validation using qRT-PCR. Total EV RNA was isolated with mirVana miRNA Isolation Kit (Ambion). The RNA samples were sent, and the microarray procedure was carried out at Exiqon Vedbaek, Denmark, as followed the previous description.[22] Briefly, the samples were labelled using the miRCURY LNA™ microRNA Hi-Power Labeling Kit, Hy3™/Hy5™ and hybridized on the miRCURY LNA™ microRNA Array (7th Gen).

2.7 | qRT-PCR

Total RNA was isolated with mirVana miRNA Isolation Kit (Ambion). Reverse transcription was performed using qScript microRNA cDNA Synthesis Kit (Quanta). PCR was performed using an ABI PRISM Sequence Detector System 7500 (Applied Biosystems) with SYBR Green (Quanta) as the fluorescent dye and ROX (Quanta) as the passive reference dye. The relative amount of each gene to U6 snRNA was used to quantify cellular RNA. The primers used for qRT-PCR were as follows:

miR-92b (forward): 5′-TAT TGC ACT CGT CCC GGC CTC C-3′
miR-139 (forward): 5′-TCT ACA GTG CAC GTG TCT CCA G-3′
miR-328 (forward): 5′-CTG GCC CTC TCT GCC CTT CCG T-3′
miR-331 (forward): 5′-CTA GGT ATG GTC CCA GGG ATC C-3′
miR-345 (forward): 5′-GCT GAC CCC TAG TCC AGT GCT T-3′
miR-378a (forward): 5′-ACT GGA CTT GGA GTC AGA AGG-3′
miR-490 (forward): 5′-CCA TGG ATC TCC AGG TGG GT-3′
miR-655 (forward): 5′-ACC AGG AGG CTG AGG TCC CT-3′
miR-767 (forward): 5′-TGC ACC ATG GTT GTC TGA GCA-3′
miR-874 (forward): 5′-CTG CCC TGG CCC GAG GGA CCG A-3′
miR-99b (forward): 5′-CAC CCG TAG AAC CGA CCT TGC G-3′
miR-124 (forward): 5′-TAA GGC ACG CGG TGA ATG CC-3′
miR-184 (forward): 5′-TGG ACG GAG AAC TGA TAA GGG T-3′
miR-200b (forward): 5′-TAA TAC TGC CTG GTA ATG ATG A-3′
miR-302a (forward): 5′-TAA GTG CTT CCA TGT TTT GGT GA-3′
miR-411 (forward): 5′-TAG TAG ACC GTA TAG CGT ACG-3′
miR-455 (forward): 5′-GCA GTC CAC GGG CAT ATA CAC-3′
miR-676 (forward): 5′-CCG TCC TGA GGT TGT TGA GCT-3′
miR-300 (forward): 5′-TAT GCA AGG GCA AGC TCT CTT C-3′
miR-204 (forward): 5′-TTC CCT TTG TCA TCC TAT GCC T-3′
miR-453 (forward): 5′-AGG TTG CCT CAT AGT GAG CTT GCA-3′
miR-3085 (forward): 5′-TCT GGC TGC TAT GGC CCC CTC-3′
miR-146a (forward): 5′-TGA GAA CTG AAT TCC ATG GGT T-3′
Reverse primer: PerfeCTa® Universal PCR Primer (Quanta)
U6 (forward): 5′-CTC GCT TCG GCA GCA CA-3′
U6 (reverse): 5′-AAC GCT TCA CGA ATT TGC GT-3′

2.8 | Bioinformatics analysis

The global UP and DOWN cardiac microRNA target genes were generated using miTarBase (Http://mitarbase.mbc.nctu.edu.tw). Bioinformatics analyses (Gene Ontology) were performed using the UniProt database and Human Protein Reference Database.23 Protein-protein interactions analyses by STRING 11.0 database with medium confidence STRING annotated interactions (STRING score > 0.4) for the bait proteins.[24] Cytoscape software (Ver 3.6.1; http://www.cytoscape.org/) was used to visualize the network.

2.9 | Statistical analysis

Where appropriate, the data are expressed as means ± s.e.m. Comparisons of the group means were made by using Student's *t* test or one-way ANOVA with a Bonferroni post-test analysis. Correlation test was performed with the Pearson's correlation coefficient measure. A *P*-value of <.05 was considered to be statistically significant.

3 | RESULTS

3.1 | Cardiac EVs from normal and failing hearts have distinctive physical and molecular signatures

Pressure overload-induced heart failure was generated in murine hearts by applying transverse aortic constriction (TAC). The cardiac EVs were isolated from normal (Sham EVs) and failing (TAC EVs) hearts using the Langendorff-based isolation followed by purification through multiple rounds of ultracentrifugations (Figure 1A). The isolated EVs were negatively stained and visualized by electron microscopy with 30 000-fold magnification. Morphological analysis revealed that EVs showed a typical cup-shaped structure with a diameter of 70 – 160 nm and that TAC EVs tended to be larger than Sham EVs (Figure 1B). Nanoparticle tracking analysis (NTA)

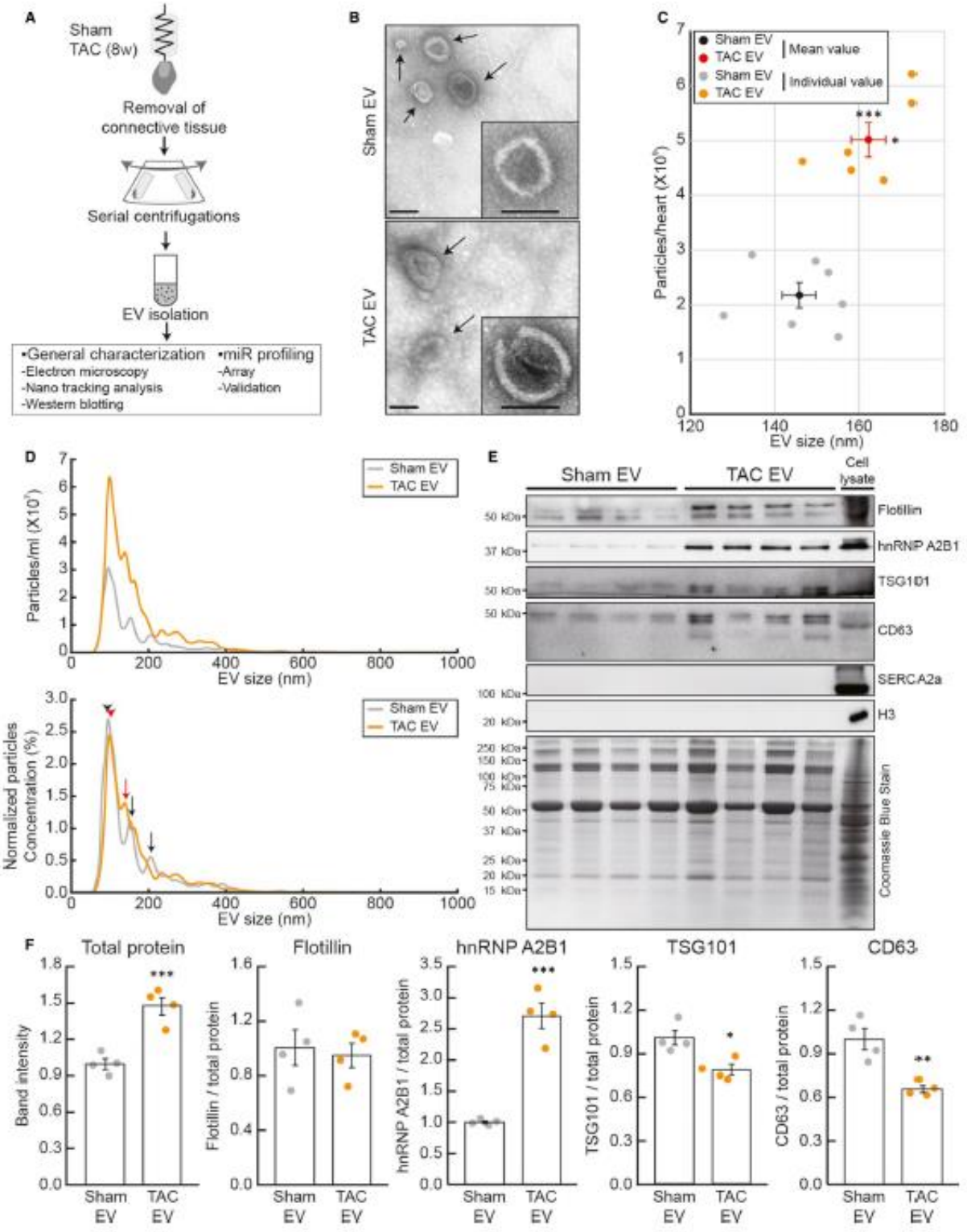
A
Sham
TAC (8w)
Removal of
connective tissue
Serial centrifugations
EV isolation
•General characterization
-Electron microscopy
-Nano tracking analysis
-Western blotting
•miR profiling
-Array
-Validation
B
Sham EV
TAC EV
C
Sham EV
TAC EV
Mean value
Sham EV
TAC EV
Individual value
Particles/heart (X10⁹)
EV size (nm)
D
Sham EV
TAC EV
Particles/ml (X10⁹)
EV size (nm)
Normalized particles
Concentration (%)
E
Sham EV
TAC EV
Cell lysate
Flotillin
hnRNP A2B1
TSG101
CD63
SERCA2a
H3
Coomassie Blue Stain
F
Total protein
Flotillin
hnRNP A2B1
TSG101
CD63
Band intensity
Flotillin / total protein
hnRNP A2B1 / total protein
TSG101 / total protein
CD63 / total protein
Sham EV
TAC EV

FIGURE 1 Characterization of in tissue cardiac EVs. A, Schematic procedure for the EV isolation. B, Representative images of electron microscopy. The bar indicates 100 nm. Arrows indicate EVs. C, Average densities and sizes of Sham and TAC EV as analysed by NTA. n = 6-7. D, Ensemble averages from several identical size distributions of Sham (n = 7) and TAC EV (n = 6). Upper: Absolute particle numbers per 1 mL, Lower: Relative concentration normalized to total nanoparticle concentrations. Arrow heads and arrows indicate the primary peak and the second or third peak, respectively. E, Representative images of Western blot and (F) quantified data. Sham EV, TAC EV and NTA indicate EVs from normal hearts, EVs from failing hearts and nanoparticle tracking analysis, respectively. *P < .05, **P < .01, ***P < .001 versus Sham EV, as determined by Student's t test. Data are presented as mean ± s.e.m

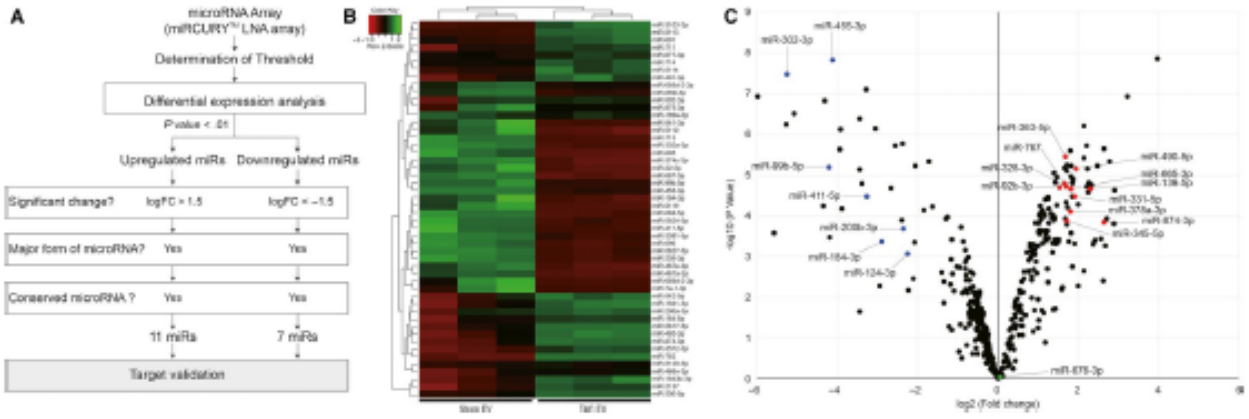

FIGURE 2 microRNA array results of tissue cardiac EVs. A, A scheme of entire procedure to identify differentially expressed microRNAs. B, Heat map and hierarchical clustering. The clustering was performed on the top 50 miRs with highest standard deviation. C, Volcano plot depicting the fold changes (*X*-axis) and *P*-value (Y-axis) in miR expression levels between Sham and TAC EV. Coloured points refer significantly up-regulated (Red), down-regulated (Blue) or unchanged (Green) microRNAs

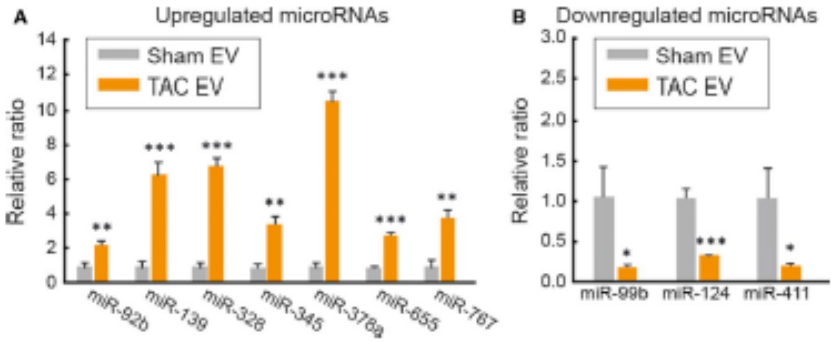

FIGURE 3 Validation of microRNA expression profiles by qRT-PCR. The levels of the up-regulated (A) or down-regulated (B) miRs were quantified by qRT-PCR. The relative levels of each microRNA were normalized to the Uó snRNA. n = 4. *P < .05, **P < .01, ***P < .001 versus Sham EV, as determined by one-way ANOVA. Data are presented as mean ± s.e.m

was performed to precisely measure the concentration and sizes of EVs. Failing hearts secrete ~5 × 10⁹ EVs per heart, whereas normal hearts release ~2 × 10⁹ EVs per heart (Figure 1C). Average size of TAC EVs was significantly larger than that of Sham EVs, which is consistent with the electron microscopic data (Figure 1D upper panel). Size distribution profiles of EVs indicated that the majority of EVs were 100 nm in size in both Sham and TAC groups. Two additional groups of Sham EVs were 150 nm and 200 nm in size. On the other hand, one group of 130 nm in size was additionally observed in TAC EVs (Figure 1D, black arrow; Sham EVs, red arrow; TAC EVs). Furthermore, Sham and TAC EVs exhibited a significant difference in their protein contents. Same volumes of EV samples (50 μL, a quarter of the total EVs from a heart) were loaded in a SDS-PAGE gel and quantified by Coomassie blue staining. In line with NTA results, 50% more proteins were detected in TAC EVs (Figure 1E and F). As shown in Figure 1F, several EV markers were analysed by Western bolt analysis. The Flotillin level was not altered between Sham and TAC EVs, but hnRNP A2B1 expression was significantly increased in TAC EVs. On the other hand, TSG101 and CDó3 expressions were substantially reduced in TAC EVs (Figure 1F). Taken together, the cardiac EVs from normal and failing hearts showed distinctive features in their physical and molecular properties.

3.2 | microRNA profiles of cardiac EVs and validation

To further characterize cardiac EVs, microRNA (miR) expression profiles were explored. Cardiac EVs were isolated from three normal and three failing hearts. All EV preparations were immediately subjected to quality control and miRNA array analyses that were conducted using the 7th generation of miRCURY™ LNA array system

(Exiqon). Of the 1,195 miRs displayed on the array, 731 miRs were eliminated due to a lack of significant signal intensity. The remaining 464 miRs were then sorted out by criteria indicated in Figure 2A (Table S1). The heat map diagram demonstrated a clear separation of miR expressions in Sham and TAC EVs (Figure 2B). Compared to Sham EVs, 107 miRs were up-regulated (23%) and 47 miRs were down-regulated (10%) in TAC EVs (Figure 2C). miRs with p-values higher than 0.05 were considered as 'not altered' (67%). The 154 miRs differentially expressed on the array were further validated for their abundancy using qRT-PCR. Consequently, we identified seven up-regulated (miR-378a, miR-665, miR-139, miR-345, miR-328, miR-767 and miR-92b) and three down-regulated (miR-99b, miR-124 and miR-411) miRs (Figure 3A and B).

3.3 | Potential target prediction for the identified miRs

To investigate the roles of the identified miRs under pathological conditions, bioinformatics analyses were performed as shown in Figure 4A (Tables 1 and 2). First, putative targets listed in miRTarBase (http://mirtarbase.mbc.nctu.edu.tw) as validated by both reporter assay and Western blot analysis were selected. Second, the selected targets were further sorted out according to their tissue distribution as reported in the proteomics database (www.proteomicsdb.org). Through these two subsequent analyses, 29 putative targets associated with the seven up-regulated miRs and 49 putative targets associated with the three down-regulated miRs were identified. Lastly, these putative targets were categorized based on their subcellular localization, biological process and protein-protein interactions (Tables 3 and 4). The analysis of subcellular localization revealed that miRs of TAC EVs appeared to target proteins predominantly located in the plasma membrane, nucleus and cytoskeleton (Figure 4B). Functional analysis suggested that target proteins for the up-regulated miRs were involved in cell cycle (19%), signal transduction (15%) and apoptosis (15%). On the other hand, intracellular targets for the down-regulated miRs were predicted to contribute to transcription/translation (22%), apoptosis (18%) and cell cycle (14%) (Figure 4 and D). The protein-protein interaction map generated by the STRING database (https://string-db.org/) is shown in Figure 5. The most frequently matched targets controlled by the up-regulated miRs in TAC EVs were NOTCH, CD44 and PTEN. Meanwhile, targets modulated by the down-regulated miRs were CDH2, GRB2 and ITGB1. Taken together, these results suggest that miRs in TAC EVs are indeed closely related to the essential biological processes.

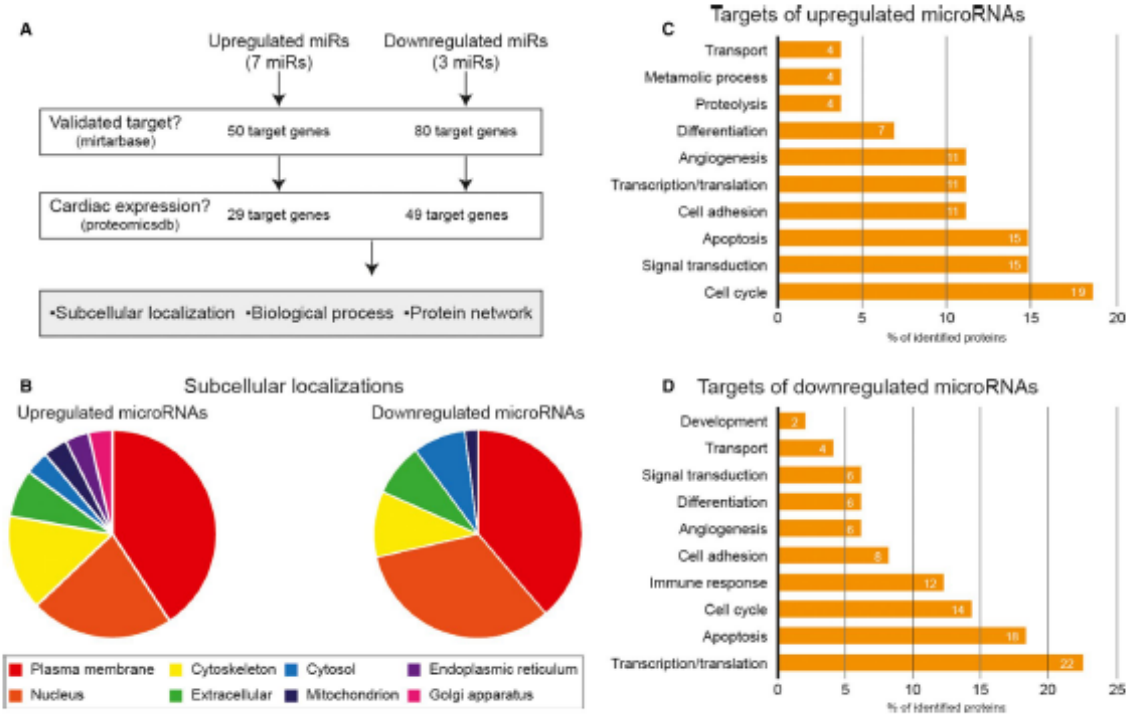

FIGURE 4 Proteomics analysis of the putative microRNA target genes. A, Analyses were conducted based on miRNA database (miRTarBase; http://mirtarbase.mbc.nctu.edu.tw) and protein database (ProteomicsDB; www.proteomicsdb.org). Target proteins were displayed by their subcellular localization (B) and Gene Ontology (GO) categories (C and D) using the STRING database (https://string-db.org/)

TABLE 1 Up-regulated miRs in TAC EV and their targets

Name	P.Value		Targets
	Microarray	qRT-PCR	
miR-767-5p	1.7E-05	0.002	
miR-328-3p	1.9E-05	1.4E-06	ABCG2, CD44, H2AFX, KCNH2, MMP16, PLCE1, SFRP1
miR-92b-3p	2.0E-05	0.004	CDKN1C, CEBPB, DAB2IP, DKK3, ITGA6, NLK, NOX4, PTEN, RECK, SLC15A1, SMAD3
miR-139-5p	2.2E-05	7.6E-05	ADGRL4, BCL2, CXCR4, FOXO1, IGF1R, IRS1, JUN, MCL1, MET, MMP11, NOTCH1, NR5A2, OIP5, PAFAH1B1, RAP1B, ROCK2, TPD52, WNT1
miR-665-3p	2.2E-05	2.6E-05	
miR-378a-3p	8.0E-05	1.0E-07	CDK6, GALNT7, IGF1R, MAPK1, NPNT, NRF1, PGR, RUNX1, TGFB2, VEGFA, VIM, WNT10A
miR-345-5p	1.3E-04	0.001	ABCC1, CDKN1A

TABLE 2 Down-regulated miRs in TAC EV and their targets

Name	P.Value		Targets
	Microarray	qRT-PCR	
miR-99b-5p	6.4E-06	0.041	ARID3A, IGF1R, MFGE8, MTOR, RAVER2
miR-124-3p	8.7E-04	1.1E-04	ABHD5, ADIPOR2, AHR, AKT2, AMOTL1, AR, B4GALT1, CAMTA1, CAV1, CBL, CCL2, CCNA2, CCND2, CD151, CDH2, CDK2, CDK4, CDK6, CEBPA, CLOCK, DLX5, E2F6, EFNB1, EGR1, EZH2, FLOT1, FOXA2, HMGA1, HNRNPA2B1, HOTAIR, IL6R, IQGAP1, ITGB1, JAG1, LAMC1, MAPK14, MTDH, MTPN, MYO10, NFATC1, NFKBIZ, NR3C1, NR3C2, PEA15, PIK3CA, PNPLA2, PPP1R13L, PRRX1, PTBP1, PTBP2, RAB38, RAP2A, RHOG, ROCK1, ROCK2, RRAS, SART3, SIRT1, SLC16A1, SMOX, SMYD3, SOS1, SPHK1, SSSCA1, STAT3, SYCP1, TRIB3, UHRF1, VAMP3, VIM
miR-411-5p	3.3E-05	0.048	GRB2

3.4 | Identification of an alternative control for miR expression

There is no clear consensus on suitable controls for relative miR quantification in circulating miRs, although U6 has been considered as an endogenous normalization control.[14–19] In this study, we tested whether U6 is an adequate control for the miR expression. U6 expression was shown to be abundant, stable and not significantly different across all 12 EV samples (Figure 6A). Therefore, U6 expression was used to normalize the qRT-PCR data presented in Figure 3. To further support and strengthen our results, we searched out potential candidates for more reliable controls that showed minimal differences in expressions between groups yet with strong signal intensity. Initial screening led us to identify five miRs, miR-676, miR-300, miR-204, miR-453 and miR-3085. Those were thoroughly tested and validated by qRT-PCR with multiple primer sets, and finally, miR-676 was selected as a new potential candidate for a EV miR expression control. As shown in Figure 6A, miR-676 indeed exhibited the most invariable expressions throughout all samples, which is comparable to U6. (Figure B and C). In fact, in regard to Ct values obtained by the Mann-Whitney test between Sham and TAC EVs, miR-676 expression ($P = .52$) was more consistent than U6 expression ($P = .11$). These data suggest that miR-676 can be used as an internal control for EV miRs with high fidelity.

4 | DISCUSSION

As EVs are highlighted as an important mediator of cell-to-cell communications during heart failure, it becomes essential to analyse the contents of cardiac EVs. In the present study, we isolated and characterized cardiac EVs from normal and failing mouse hearts. In the physical and molecular analyses, TAC EVs showed distinctive features in terms of density, size, protein expression patterns and miR contents as compared to those from Sham EVs (Figure 1). EVs are bound to cell surface proteins, extracellular matrix (ECM) molecules and components of the blood plasma through its surface molecules, and located in the niche of ECM or plasma.[25] Several studies have characterized circulating EVs or miRs during cardiac diseases, but available

TABLE 3 Putative targets of the up-regulated miRs and their localization, biological process and cardiac expression

Up-regulated microRNAs					
Target Genes	**Primary Localization**	**Primary Biological Process**	**Cardiac Expression**	**Expression in Failing Heart**	**Reference**
miR-92b-3p					
CDKN1C	Nucleus	Cell cycle	4.36	Down	[53]
CEBPB	Nucleus	Transcription and translation	4.63	Down	[55]
DAB2IP	Plasma membrane	Angiogenesis	3.74	No study	
DKK3	Extracellular	Signal transduction	4.03	Down	[54]
ITGA6	Plasma membrane	Cell adhesion	4.35	No study	
PTEN	Plasma membrane	Apoptosis	4.43	Down	[52]
RECK	Plasma membrane	Angiogenesis	3.34	No study	
SMAD3	Nucleus	Transcription and translation	4.17	Up	[59]
miR-139-5p					
BCL2	Cytosol	Apoptosis	3.94	Down	[56]
IGF1R	Plasma membrane	Signal transduction	3.98	Up	[41]
MCL1	Mitochondrion	Apoptosis	3.42	Down	[57]
NOTCH1	Nucleus	Angiogenesis	2.97	Up	[60]
PAFAH1B1	Cytoskeleton	Cell cycle	5.44	No study	
RAP1B	Plasma membrane	Signal transduction	5.47	No study	
ROCK2	Plasma membrane	Apoptosis	4.38	Up	[42]
TPD52	Endoplasmic reticulum	Differentiation	4.97	No study	
miR-328-3p					
CD44	Plasma membrane	Cell adhesion	4.3	Up	[61]
H2AFX	Nucleus	Cell cycle	4.6	No study	
MMP16	Plasma membrane	Proteolysis	3.08	No study	
SFRP1	Plasma membrane	Differentiation	4.88	No change	
miR-345-5p					
ABCC1	Plasma membrane	Transport	3.66	No study	
miR-378a-3p					
CDK6	Cytoskeleton	Cell cycle	5.01	No study	
GALNT7	Golgi apparatus	Metabolic process	2.89	No study	
IGF1R	Plasma membrane	Signal transduction	3.98	Up	[41]
MAPK1	Cytoskeleton	Apoptosis	5.14	Up	[35]
NPNT	Extracellular	Cell adhesion	4.05	No study	
Nrf1	Nucleus	Transcription and translation	4.29	Up	[62]
VIM	Cytoskeleton	Signal transduction	7.38	Up	[47]

information was highly limited since most of the studies were conducted using blood plasma.[26,27] Recently, Loyer X. et al investigated cardiac EVs in the model of myocardial infarction.[28] In their report, they minced ventricles to obtain cardiac EVs, which might damage cardiac cells and increase potential contaminants from other intracellular components. In our study, on a contrary, Langendorff-based EV isolation was employed to minimize damaging cells (Figure 1A). In addition, we have also compared our data with a previous study about the circulating miRs in a canine heart failure model.[27] However, only thirteen miRs were confirmed to be identical out of fifty seven miRs reported in this paper (Table S1). This weak correlation suggests distinctive miR profiles of EVs in the ECM and plasma, which is probably due to different cellular origins of EVs. Plasma EVs could be released from the other organ or tissues, but EVs used for our study is strictly from cardiac tissues. In a similar context, we found the different size distribution and protein profiles between Sham and TAC EVs (Figure 1D-F). In fact, our NTA data showed that the size of EVs in HF is larger than that of Sham. Previously, Minghua et al showed that

TABLE 4 Putative targets of the down-regulated miRs and their localization, biological process and cardiac expression

Down-regulated microRNAs					
Target Genes	**Primary Localization**	**Primary Biological Process**	**Cardiac Expression**	**Expression in Failing Heart**	**Reference**
miR-99b-5p					
ARID3A	Nucleus	Transcription and translation	3.08	No Study	
IGF1R	Plasma membrane	Immune response	3.98	Up	[41]
MFGE8	Cytoskeleton	Angiogenesis	4.51	Down	[63]
MTOR	Nucleus	Cell cycle	3.48	up	[46]
miR-124-3p					
ABHD5	Cytosol	Differentiation	2.66	Down	[64]
AKT2	Nucleus	Apoptosis	3.87	No Study	
AMOTL1	Cytosol	Angiogenesis	2.88	No Study	
B4GALT1	Plasma membrane	Development	3.79	No Study	
CAV1	Plasma membrane	Immune response	6.78	Down	[65]
CBL	Golgi apparatus	Signal transduction	3.59	Up	[50]
CD151	Plasma membrane	Cell adhesion	4.82	Controversial	
CDH2	Plasma membrane	Cell adhesion	5.96	Up	[43]
CDK2	Nucleus	Cell cycle	4.34	UP	[48]
CDK4	Nucleus	Cell cycle	4.11	No change	[66]
CDK6	Nucleus	Cell cycle	5.01	No Study	
EFNB1	Plasma membrane	Differentiation	4.42	No study	
FLOT1	Plasma membrane	Immune response	5.34	No Study	
HMGA1	Nucleus	Transcription and translation	5.49	Down	[67]
HNRNPA2B1	Extracellular	Transcription and translation	6.57	No Study	
IQGAP1	Plasma membrane	Immune response	4.56	No Study	
ITGB1	Plasma membrane	Cell adhesion	5.68	No Study	
LAMC1	Extracellular	Cell adhesion	6.25	No Study	
MAPK14	Nucleus	Apoptosis	4.97	Up	[44]
MTDH	Nucleus	Apoptosis	4.25	No Study	
MTPN	Cytoskeleton	Transcription and translation	5.6	No Study	
NR3C1	Nucleus	Apoptosis	4.26	No Study	
PEA15	Cytoskeleton	Apoptosis	5.43	No Study	
PIK3CA	Cytosol	Angiogenesis	2.89	Up	[51]
PPP1R13L	Extracellular	Apoptosis	4.06	No Study	
PRRX1	Nucleus	Transcription and translation	4.03	No Study	
PTBP1	Nucleus	Transcription and translation	5.69	No Study	
PTBP2	Nucleus	Transcription and translation	4.98	No Study	
RAP2A	Plasma membrane	Signal transduction	4.3	No Study	
RHOG	Plasma membrane	Transcription and translation	5.07	No Study	
ROCK1	Cytoskeleton	Apoptosis	4.25	UP	[42]
ROCK2	Plasma membrane	Apoptosis	4.38	UP	[42]
RRAS	Plasma membrane	Differentiation	5.33	No Study	
SART3	Nucleus	Transcription and translation	4.07	Up	[45]
SIRT1	Nucleus	Apoptosis	3.37	Up	[49]
SLC16A1	Plasma membrane	Transport	5.16	No Study	
SMYD3	Nucleus	Transcription and translation	3.99	No Study	

(Continues)

TABLE 4 (Continued)

Down-regulated microRNAs					
Target Genes	Primary Localization	Primary Biological Process	Cardiac Expression	Expression in Failing Heart	Reference
SOS1	Cytosol	Immune response	3.31	No Study	
SSSCA1	Extracellular	Cell cycle	4.74	No Study	
STAT3	Nucleus	Transcription and translation	4.91	Up	[40]
SYCP1	Nucleus	Cell cycle	4.27	No Study	
UHRF1	Nucleus	Cell cycle	4.04	No Study	
VAMP3	Plasma membrane	Transport	4.88	No Study	
VIM	Cytoskeleton	Immune response	7.38	Up	[47]
miR-411-5p					
GRB2	Plasma membrane	Signal transduction	5.19	No Study	

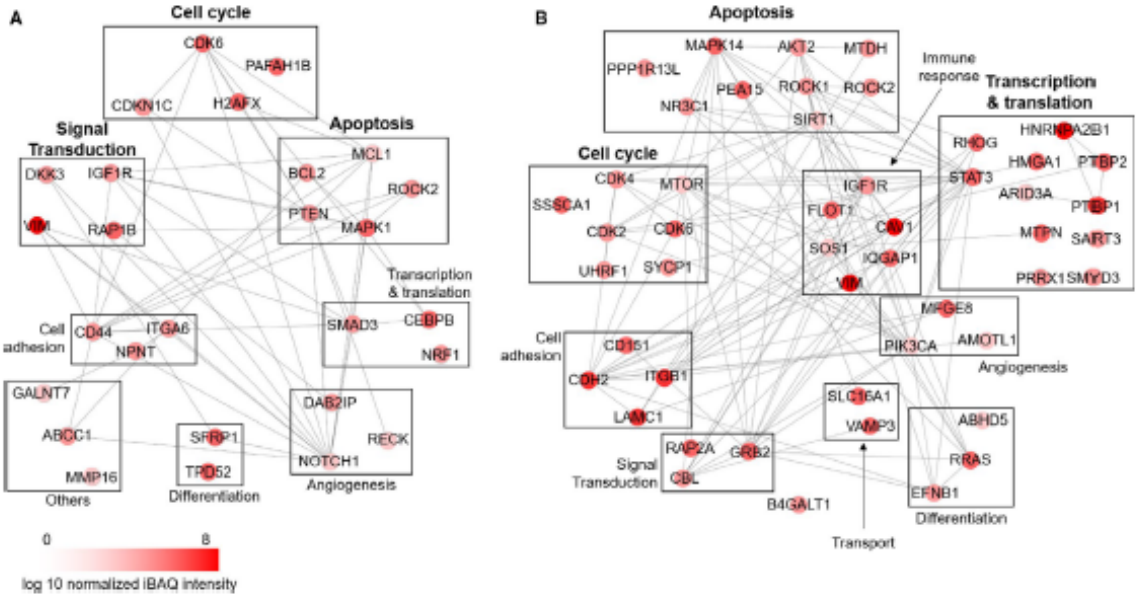

FIGURE 5 In silico protein-protein interaction map for putative microRNA targets. The protein-protein maps were constructed using STRING 11.0 database and Cytoscape. The putative molecular targets by up-regulated microRNAs (A) and down-regulated microRNAs (B). The iBAQ intensity represents the expression level of proteins in the heart

size of exosomes were changed in remote ischaemic preconditioning-mediated cardioprotection,[28] which is correlated with our morphological observations. Taken together, these differences are also presumably related to the dynamic changes in the cellular composition of the heart under pathological conditions. In addition, we also observed the differences in the expression of exosomal markers. For example, CD63 and TSG101 were decreased in TAC EVs and these markers were previously reported to be involved in cardiac fibrosis and hypertrophy, respectively.[29,30] On the other hand, hnRNP A2B1 expression was increased and this was known to control the sorting of miRs into exosomes through specific binding motif.[31] Although we particularly focused on miR profiles in EVs, this result also suggests a possibility that proteins in EVs could actively regulate cardiac intercellular communication.

From EV miR profiles, we have identified seven up-regulated and three down-regulated miRs in failing hearts compared to controls. Briefly, miR-757, miR-328, miR-92b, miR-139, miR-665, miR-378a and miR-345 were up-regulated, whereas, miR-99b, miR-124 and miR-411 were down-regulated during heart failure (Tables 1 and 2). Among the seven up-regulated miRs, three miRs (miR-92b, miR-139 and miR-378a) are known to be anti-hypertrophic[31–34] and another three miRs (miR-139, miR-378a and miR-345) are anti-fibrotic[35–37] (Table 5). These data indicate that up-regulated miRs are likely involved in the cardioprotective function. Interestingly, one

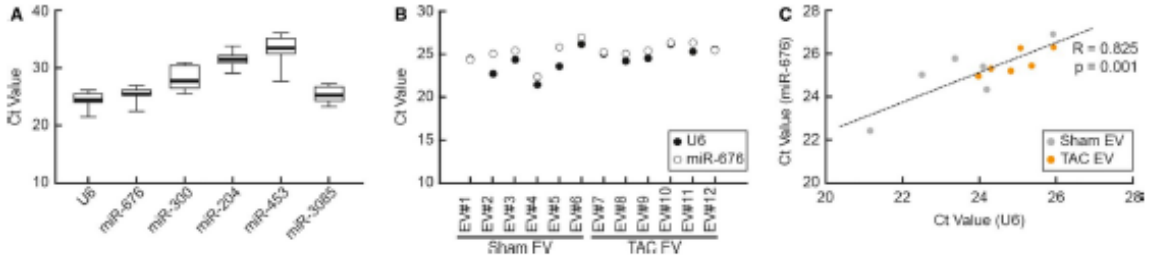

FIGURE 6 Identification of internal microRNA control. A, The Ct values of U6 and microRNA candidates as an internal control were quantified by qRT-PCR. n = 12, data are presented as mean ± s.e.m. B, The Ct values of U6 and miR-676 in entire 12 samples were presented. C, The Pearson correlation coefficient was used to measure the strength of a linear association between U6 and miR-676 expressions. $R = 0.825$, $P = .001$

of down-regulated miRs, miR-124, is also known to induce cardiac hypertrophy,[58] attenuate cardiac function and stimulate angiogenesis.[59] Therefore, EV miRs released from failing hearts may play important roles in cardioprotection (Table 5). On the other hand, a negative-inotropic miR, miR-328, was found to be increased and an anti-fibrotic miR, miR-411, was decreased. In addition, we evaluated EV miR-146a, a negative-inotropic miR, that we previously reported,[10] as a positive control and it was also significantly increased (Figure S1). Therefore, even though anti-hypertrophic and anti-fibrotic EV miRs are mainly elevated in TAC EVs, the negative-inotropic and pro-fibrotic miRs are also enriched. These ambivalent features of TAC EVs may result from diverse cellular origins of EVs, and EV miRs are meticulously balanced in normal heart. This finding is in line with the previous reports that EVs from cardiac stem cells are normally salubrious and the EVs from fibroblasts and endothelial cells are deleterious.[4,8–10,12]

Furthermore, bioinformatics was applied as an alternative approach to predict the impact of EV miRs on cardiac function. First, we predicted the possible cardiac outcomes with previously reported targets for miRs identified in this study. Next, we performed literature studies and compared with previous results. In brief, molecular targets experimentally validated by both a reporter assay and Western blot analysis were initially selected based on the miR database (miRTarBase) and 52 targets that are not expressed in the heart were discarded. The remaining 77 putative targets of EV miRs are summarized in Table 3 (targets for up-regulated miRs) and Table 4 (targets for down-regulated miRs). Intriguingly, approximately 72% of targets anticipated to be up-regulated were confirmed to be elevated indeed in diseased conditions by previous reports,[40–51] and 50% of targets expected to be down-regulated were actually reduced.[52–57] This result proves that EV miRs from failing hearts substantially affect gene expressions in the heart.

Lastly, there have been controversial reports for the usage of U6 although it is the most frequently used endogenous reference control.[14–19] For example, U6 expression was not stable in tissues or plasma from patients with cancer.[14,15,17] Therefore, we deliberated an extra assessment for the evaluation of EV miR expression. Initially, U6 was confirmed to be abundant and stable in our samples and used as a reference control in this study. To avoid potential critics for the usage of U6, we decided to identify alternative reference miR. Through the miRNA profile analysis, miR-676 was appeared as a promising candidate due to its superior abundance and stability. Upon this result, additional normalization was performed using miR-676 (Figure S2) and a significant correlation between U6 and miR-676 was confirmed. Although miR-676 is reported to be elevated in the liver in the response to a high-fat diet,[58] there are no reports relating to cardiac function. Therefore, miR-676 may be a suitable reference in EV miR research although further validations are necessary in various cardiac diseases.

TABLE 5 Previously described functions of differentially expressed miRs in TAC EV

Name	Contractility	Hypertrophy	Fibrosis	Reference
Up-regulated microRNAs				
miR-92b	Unknown	↓	-	[33]
miR-139	Unknown	↓	↓	[32,36]
miR-378a	Unknown	↓	↓	[34,35]
miR-345	Unknown	Unknown	↓	[37]
miR-328	↓	↑	↑	[68,69]
Down-regulated microRNAs				
miR-124	↓	↑		[38,39]
miR-411	Unknown	Unknown	↓	[70]

I.

In summary, we isolated and characterized cardiac EVs in the context of miR contents using normal and failing hearts. EVs from both hearts exhibited substantial contrasts in physical and functional features. We also found that EVs from failing hearts contains both beneficial and detrimental miRs presumably because current EV miR profiles that we reported here were generated from mixed cellular origins in failing hearts, which is a limitation of this study.

Taken together, our study shows dynamic intercellular communications via EV miRs during heart failure and it will be critical to identify the origin of beneficial EVs for a therapeutic application to treat heart failure.

ACKNOWLEDGEMENTS

This work is supported by The Assistant Secretary of Defense for Health Affairs endorsed by the Department of Defense, through the FY17, DMDRP, Career Development Award programme under Award No. W81XWH-18-1-0322. C. K was supported by the American Heart Association (AHA) 18TPA34170460 and the Assistant Secretary of Defense for Health Affairs endorsed by the Department of Defense, through the FY18, CDMRP, Investigator-Initiated Research Award: No. W81XWH-19-1-0382.

CONFLICT OF INTEREST

The authors declare that they have no conflicts of interest.

AUTHOR CONTRIBUTIONS

JGO, PL and DJ designed the research, performed the experiments, analysed the data and wrote the paper. REG contributed in performing EM microscopy. SS and CK served as scientific advisor. DJ revised a manuscript and data.

DATA AVAILABILITY STATEMENT

All data generated or analysed during this study are included in this published article (and its supplementary information files). Furthermore, the raw data sets generated during the current study are also available from the corresponding author on reasonable request.

ORCID

Dongtak Jeong https://orcid.org/0000-0003-4153-3498

REFERENCES

1. Zhou P, Pu WT. Recounting cardiac cellular composition. *Circ Res*. 2017;118(3):368-370.
2. Rienks M, Papageorgiou AP, Frangogiannis NG, Heymans S. Myocardial extracellular matrix: an ever-changing and diverse entity. *Circ Res*. 2014;114(5):872-888.
3. Tian Y, Morrisey EE. Importance of myocyte-nonmyocyte interactions in cardiac development and disease. *Circ Res*. 2012;110(7):1023-1034.
4. Bang C, Antoniades C, Antonopoulos AS, et al. Intercellular communication lessons in heart failure. *Eur J Heart Fail*. 2015;17(11):1091-1103.
5. Valadi H, Ekstrom K, Bossios A, Sjostrand M, Lee JJ, Lotvall JO. Exosome-mediated transfer of mRNAs and microRNAs is a novel mechanism of genetic exchange between cells. *Nat Cell Biol*. 2007;9(6):654-659.
6. Tachibana A, Santoso MR, Mahmoudi M, et al. Paracrine effects of the pluripotent stem cell-derived cardiac myocytes salvage the injured myocardium. *Circ Res*. 2017;121(6):e22-e36.
7. Gallet R, Dawkins J, Valle J, et al. Exosomes secreted by cardiosphere-derived cells reduce scarring, attenuate adverse remodelling, and improve function in acute and chronic porcine myocardial infarction. *Eur Heart J*. 2017;38(3):201-211.
8. Agarwal U, George A, Bhutani S, et al. Experimental, systems, and computational approaches to understanding the microRNA-mediated reparative potential of cardiac progenitor cell-derived exosomes from pediatric patients. *Circ Res*. 2017;120(4):701-712.
9. Khan M, Nickoloff E, Abramova T, et al. Embryonic stem cell-derived exosomes promote endogenous repair mechanisms and enhance cardiac function following myocardial infarction. *Circ Res*. 2015;117(1):52-64.
10. Oh JG, Watanabe S, Lee A, et al. miR-146a ssuppresses SUMO1 expression and induces cardiac dysfunction in maladaptive hypertrophy. *Circ Res*. 2018;123(6):673-685.
11. Bang C, Batkai S, Dangwal S, et al. Cardiac fibroblast-derived microRNA passenger strand-enriched exosomes mediate cardiomyocyte hypertrophy. *J Clin Invest*. 2014;124(5):2136-2146.
12. Halkein J, Tabruyn SP, Ricke-Hoch M, et al. MicroRNA-146a is a therapeutic target and biomarker for peripartum cardiomyopathy. *J Clin Invest*. 2013;123(5):2143-2154.
13. Loyer X, Zlatanova I, Devue C, et al. Intra-cardiac release of extracellular vesicles shapes inflammation following myocardial infarction. *Circ Res*. 2018;123(1):100-106.
14. Gouin K, Peck K, Antes T, et al. A comprehensive method for identification of suitable reference genes in extracellular vesicles. *J Extracell Vesicles*. 2017;6(1):1347019.
15. Xiang M, Zeng Y, Yang R, et al. U6 is not a suitable endogenous control for the quantification of circulating microRNAs. *Biochem Biophys Res Commun*. 2014;454(1):210-214.
16. Chen ZH, Zhang GL, Li HR, et al. A panel of five circulating microRNAs as potential biomarkers for prostate cancer. *Prostate*. 2012;72(13):1443-1452.
17. Peltier HJ, Latham GJ. Normalization of microRNA expression levels in quantitative RT-PCR assays: identification of suitable reference RNA targets in normal and cancerous human solid tissues. *RNA*. 2008;14(5):844-852.
18. Davoren PA, McNeill RE, Lowery AJ, Kerin MJ, Miller N. Identification of suitable endogenous control genes for microRNA gene expression analysis in human breast cancer. *BMC Mol Biol*. 2008;9:76.
19. Chen X, Ba Y, Ma L, et al. Characterization of microRNAs in serum: a novel class of biomarkers for diagnosis of cancer and other diseases. *Cell Res*. 2008;18(10):997-1006.
20. Ishiguro K, Yan IK, Patel T. Isolation of tissue extracellular vesicles from the Liver. *J Viz Exp*. 2019.
21. Alexander M, Hu R, Runtsch MC, et al. Exosome-delivered microRNAs modulate the inflammatory response to endotoxin. *Nat Commun*. 2015;6:7321.
22. Castoldi M, Schmidt S, Benes V, et al. A sensitive array for microRNA expression profiling (miChip) based on locked nucleic acids (LNA). *RNA*. 2006;12(5):913-920.
23. Keshava Prasad TS, Goel R, Kandasamy K, et al. Human protein reference database--2009 update. *Nucleic Acids Res*. 2009;37(Database):D767-D772.
24. Jensen LJ, Kuhn M, Stark M, et al. STRING 8--a global view on proteins and their functional interactions in 630 organisms. *Nucleic Acids Res*. 2009;37(Database):D412-D416.

25. Buzas EI, Toth EA, Sodar BW, Szabo-Taylor KE. Molecular interactions at the surface of extracellular vesicles. *Semin Immunopathol*. 2018;40(5):453-464.
26. Gidlof O, Evander M, Rezeli M, Marko-Varga G, Laurell T, Erlinge D. Proteomic profiling of extracellular vesicles reveals additional diagnostic biomarkers for myocardial infarction compared to plasma alone. *Sci Rep*. 2019;9(1):8991.
27. Yang VK, Loughran KA, Meola DM, et al. Circulating exosome microRNA associated with heart failure secondary to myxomatous mitral valve disease in a naturally occurring canine model. *J Extracell Vesicles*. 2017;6(1):1350088.
28. Minghua W, Zhijian G, Chahua H, et al. Plasma exosomes induced by remote ischaemic preconditioning attenuate myocardial ischaemia/reperfusion injury by transferring miR-24. *Cell Death Dis*. 2018;9(3):320.
29. Takawale A, Zhang P, Patel VB, Wang X, Oudit G, Kassiri Z. Tissue inhibitor of matrix metalloproteinase-1 promotes myocardial fibrosis by mediating CD63-Integrin beta1 interaction. *Hypertension*. 2017;69(6):1092-1103.
30. Essandoh K, Deng S, Wang X, et al. Tsg101 positively regulates physiologic-like cardiac hypertrophy through FIP3-mediated endosomal recycling of IGF-1R. *FASEB J*. 2019;33(6):7451-7466.
31. Villarroya-Beltri C, Gutierrez-Vazquez C, Sanchez-Cabo F, et al. Sumoylated hnRNPA2B1 controls the sorting of miRNAs into exosomes through binding to specific motifs. *Nat Commun*. 2013;4:2980.
32. Ming S, Shui-Yun W, Wei Q, et al. miR-139-5p inhibits isoproterenol-induced cardiac hypertrophy by targetting c-Jun. *Biosci Rep*. 2018;38(2).
33. Hu ZQ, Luo JF, Yu XJ, et al. Targeting myocyte-specific enhancer factor 2D contributes to the suppression of cardiac hypertrophic growth by miR-92b-3p in mice. *Oncotarget*. 2017;8(54):92079-92089.
34. Ganesan J, Ramanujam D, Sassi Y, et al. MiR-378 controls cardiac hypertrophy by combined repression of mitogen-activated protein kinase pathway factors. *Circulation*. 2013;127(21):2097-2106.
35. Yuan J, Liu H, Gao W, et al. MicroRNA-378 suppresses myocardial fibrosis through a paracrine mechanism at the early stage of cardiac hypertrophy following mechanical stress. *Theranostics*. 2018;8(9):2565-2582.
36. Jiang C, Tong Z, Fang WL, et al. Microrna-139-5p inhibits epithelial-mesenchymal transition and fibrosis in post-menopausal women with interstitial cystitis by targeting LPAR4 via the PI3K/Akt signaling pathway. *J Cell Biochem*. 2018;119(8):6429-6441.
37. Chen W, Zhao W, Yang A, et al. Integrated analysis of microRNA and gene expression profiles reveals a functional regulatory module associated with liver fibrosis. *Gene*. 2017;636:87-95.
38. Zhao Y, Yan M, Chen C, et al. MiR-124 aggravates failing hearts by suppressing CD151-facilitated angiogenesis in heart. *Oncotarget*. 2018;9(18):14382-14396.
39. Bao Q, Chen L, Li J, et al. Role of microRNA-124 in cardiomyocyte hypertrophy inducedby angiotensin II. *Cell Mol Biol (Noisy-le-grand)*. 2017;63(4):23-27.
40. Cai K, Chen H. MiR-625-5p inhibits cardiac hypertrophy through targeting STAT3 and CaMKII. *Hum Gene Ther Clin Dev*. 2019.
41. Batlle M, Castillo N, Alcarraz A, et al. Axl expression is increased in early stages of left ventricular remodeling in an animal model with pressure-overload. *PLoS ONE*. 2019;14(6):e0217926.
42. Sunamura S, Satoh K, Kurosawa R, et al. Different roles of myocardial ROCK1 and ROCK2 in cardiac dysfunction and postcapillary pulmonary hypertension in mice. *Proc Natl Acad Sci USA*. 2018;115(30):E7129-E7138.
43. Derda AA, Woo CC, Wongsurawat T, et al. Gene expression profile analysis of aortic vascular smooth muscle cells reveals upregulation of cadherin genes in myocardial infarction patients. *Physiol Genomics*. 2018;50(8):648-657.
44. Rose BA, Yokota T, Chintalgattu V, et al. Cardiac myocyte p38alpha kinase regulates angiogenesis via myocyte-endothelial cell crosstalk during stress-induced remodeling in the heart. *J Biol Chem*. 2017;292(31):12787-12800.
45. Han Y, Wang Q, Fan X, et al. Epigallocatechin gallate attenuates overload-induced cardiac ECM remodeling via restoring T cell homeostasis. *Mol Med Rep*. 2017;16(3):3542-3550.
46. Li Q, Xie J, Wang B, et al. Overexpression of microRNA-99a attenuates cardiac hypertrophy. *PLoS ONE*. 2016;11(2):e0148480.
47. Jeong D, Lee MA, Li Y, et al. Matricellular protein CCN5 reverses established cardiac fibrosis. *J Am Coll Cardiol*. 2016;67(13):1556-1568.
48. Yu Z, Zhang H, Yu M, Ye Q. Analysis of gene expression during the development of congestive heart failure after myocardial infarction in rat models. *Int Heart J*. 2015;56(4):444-449.
49. Oka S, Zhai P, Yamamoto T, et al. Peroxisome proliferator activated receptor-alpha association with silent information regulator 1 suppresses cardiac fatty acid metabolism in the failing heart. *Circ Heart Fail*. 2015;8(6):1123-1132.
50. Rafiq K, Kolpakov MA, Seqqat R, et al. c-Cbl inhibition improves cardiac function and survival in response to myocardial ischemia. *Circulation*. 2014;129(20):2031-2043.
51. Perrino C, Naga Prasad SV, Schroder JN, Hata JA, Milano C, Rockman HA. Restoration of beta-adrenergic receptor signaling and contractile function in heart failure by disruption of the betaARK1/phosphoinositide 3-kinase complex. *Circulation*. 2005;111(20):2579-2587.
52. Nie X, Fan J, Li H, et al. miR-217 promotes cardiac hypertrophy and dysfunction by targeting PTEN. *Mol Ther Nucleic Acids*. 2018;12:254-266.
53. Lalem T, Zhang L, Scholz M, et al. Cyclin dependent kinase inhibitor 1 C is a female-specific marker of left ventricular function after acute myocardial infarction. *Int J Cardiol*. 2018;274:319-325.
54. Cao Q, Zhang J, Gao L, Zhang Y, Dai M, Bao M. Dickkopf3 upregulation mediates the cardioprotective effects of curcumin on chronic heart failure. *Mol Med Rep*. 2018;17(5):7249-7257.
55. Tie Y, Zhai C, Zhang Y, et al. CCAAT/enhancer-binding protein beta overexpression alleviates myocardial remodelling by regulating angiotensin-converting enzyme-2 expression in diabetes. *J Cell Mol Med*. 2017;22(3):1475-1488.
56. Wu C, Dong S, Li Y. Effects of miRNA-455 on cardiac hypertrophy induced by pressure overload. *Int J Mol Med*. 2015;35(4):893-900.
57. Thomas RL, Roberts DJ, Kubli DA, et al. Loss of MCL-1 leads to impaired autophagy and rapid development of heart failure. *Genes Dev*. 2013;27(12):1365-1377.
58. Awazawa M, Gabel P, Tsaousidou E, et al. A microRNA screen reveals that elevated hepatic ectodysplasin A expression contributes to obesity-induced insulin resistance in skeletal muscle. *Nat Med*. 2017;23(12):1466-1473.
59. Zhang WW, Bai F, Wang J, et al. Edaravone inhibits pressure overload-induced cardiac fibrosis and dysfunction by reducing expression of angiotensin II AT1 receptor. *Drug Des Devel Ther*. 2017;11:3019-3033.
60. Khandekar A, Springer S, Wang W, et al. Notch-mediated epigenetic regulation of voltage-gated potassium currents. *Circ Res*. 2016;119(12):1324-1338.
61. Salvador AM, Nevers T, Velazquez F, et al. Intercellular adhesion molecule 1 regulates left ventricular leukocyte infiltration, cardiac remodeling, and function in pressure overload-induced heart failure. *J Am Heart Assoc*. 2016;5(3):e003126.
62. Watanabe S, Horie T, Nagao K, et al. Cardiac-specific inhibition of kinase activity in calcium/calmodulin-dependent protein kinase kinase-beta leads to accelerated left ventricular remodeling and

heart failure after transverse aortic constriction in mice. *PLoS ONE*. 2014;9(9):e108201.
63. Deng KQ, Li J, She ZG, et al. Restoration of circulating MFGE8 (Milk Fat globule-EGF Factor 8) attenuates cardiac hypertrophy through inhibition of akt pathway. *Hypertension*. 2017;70(4):770-779.
64. Jebessa ZH, Shanmukha Kumar D, Dewenter M, et al. The lipid droplet-associated protein ABHD5 protects the heart through proteolysis of HDAC4. *Nat Metab*. 2019;1(11):1157-1167.
65. Bryant SM, Kong CHT, Watson JJ, et al. Caveolin 3-dependent loss of t-tubular ICa during hypertrophy and heart failure in mice. *Exp Physiol*. 2018;103(5):652-665.
66. Mohamed TMA, Ang YS, Radzinsky E, et al. Regulation of cell cycle to stimulate adult cardiomyocyte proliferation and cardiac regeneration. *Cell*. 2018;173(1) :104-116.e12.
67. You XY, Huang JH, Liu B, Liu SJ, Zhong Y, Liu SM. HMGA1 is a new target of miR-195 involving isoprenaline-induced cardiomyocyte hypertrophy. *Biochemistry (Mosc)*. 2014;79(6):538-544.
68. Du W, Liang H, Gao X, et al. MicroRNA-328, a potential anti-fibrotic target in cardiac interstitial fibrosis. *Cell Physiol Biochem*. 2018;39(3):827-836.
69. Li C, Li X, Gao X, et al. MicroRNA-328 as a regulator of cardiac hypertrophy. *Int J Cardiol*. 2014;173(2):268-276.
70. Ai P, Shen B, Pan H, Chen K, Zheng J, Liu F. MiR-411 suppressed vein wall fibrosis by downregulating MMP-2 via targeting HIF-1alpha. *J Thromb Thrombolysis*. 2018;45(2):264-273.

SUPPORTING INFORMATION

Additional supporting information may be found online in the Supporting Information section.

How to cite this article: Oh JG, Lee P, Gordon RE, Sahoo S, Kho C, Jeong D. Analysis of extracellular vesicle miRNA profiles in heart failure. *J Cell Mol Med*. 2020;24:7214–7227. https://doi.org/10.1111/jcmm.15251

II. Lee MA, Raad N, Song MH, Yoo J, Lee M, Jang SP, Kwak TH, Kook H, Choi E, Cha T, Hajjar RJ, **Jeong D****, Park WJ**. The matricellular protein CCN5 prevents adverse atrial structural and electrical remodeling. ***J Cell Mol Med. 2020 July 30 (in press)***

Acceptance letter from JCMM editor

Dear Dongtak Jeong,

Article ID: JCMM15789
Article DOI: 10.1111/jcmm.15789
Internal Article ID: 16863297
Article: The matricellular protein CCN5 prevents adverse atrial structural and electrical remodeling
Journal: Journal of Cellular and Molecular Medicine

Congratulations on the acceptance of your article for publication in Journal of Cellular and Molecular Medicine.

Your article has been received and the production process is now underway. We look forward to working with you and publishing your article. Using Wiley Author Services, you can track your article's progress.

Please click below to login - if you are using a different email address than this one, you will need to manually assign this article to your Dashboard (see How do I assign a missing article to My Dashboard?):

https://authorservices.wiley.com/index.html#login?campaign=email_invitation-new

If applicable, a list of available actions will appear below – check out your Author Services Dashboard for all actions related to your articles.

Track your article's progress to publication
Access your published article

If you need any assistance, please click here to view our Help section.

Sincerely,
Wiley Author Services

The matricellular protein CCN5 prevents adverse atrial structural and electrical remodeling

Min-Ah Lee, PhD[1,*], Nour Raad, MD, PhD[2,*], Min Ho Song, BS[1,*], Jimeen Yoo, MS[2], Miyoung Lee, BS[1], Seung Pil Jang, PhD[3], Tae Hwan Kwak, MS[3], Hyun Kook, MD, PhD[4], Eun-Kyoung Choi, MS[5], Tae-Joon Cha, MD, PhD[5], Roger J. Hajjar, MD[6], Dongtak Jeong, PhD[2,7,**], Woo Jin Park, PhD[1,3,**]

[1] College of Life Sciences, Gwangju Institute of Science and Technology, Gwangju, Republic of Korea

[2] Cardiovascular Research Center, Icahn School of Medicine at Mount Sinai, New York, New York, USA

[3]Bethphagen, S3-203, Gwangju Institute of Science and Technology, Gwangju, Republic of Korea

[4]Basic Research Laboratory, Chonnam National University Medical School, Hwasun-gun, Jeollanam-do, Republic of Korea

[5]Division of Cardiology, Kosin University Gospel Hospital, Busan, Republic of Korea

[6]Phospholamban Foundation, Amsterdam, Netherlands.

[7]Department of Molecular and Life Science, College of Science and Convergence Technology, Hanyang University ERICA Campus, Ansan, Gyeonggi-do, Republic of Korea

*These authors contribute equally to this study.

Addresses for correspondence:

**Woo Jin Park, PhD, College of Life Sciences, Gwangju Institute of Science and Technology (GIST), 123 Cheomdangwagi-ro, Buk-gu, Gwangju 61005, South Korea.
Tel.: +82-10-2607-2491; Fax: +82-62-715-2484; E-mail: woojinpark@icloud.com.

**Dongtak Jeong, PhD, Department of Molecular and Life Science, College of Science and Convergence Technology, Hanyang University ERICA Campus, 55 Hanyangdeahak-ro, Sangnok-gu, Ansan, Gyeonggi-do, 15588, Korea
E-mail: cooljdt@hanyang.ac.kr

Abstract

Atrial structural remodeling including atrial hypertrophy and fibrosis is a key mediator of atrial fibrillation (AF). We previously demonstrated that the matricellular protein CCN5 elicits anti-fibrotic and anti-hypertrophic effects in left ventricles under pressure overload. We here determined the utility of CCN5 in ameliorating adverse atrial remodeling and arrhythmias in a murine model of angiotensin II (AngII) infusion. Advanced atrial structural remodeling was induced by AngII infusion in control mice and mice overexpressing CCN5 either through transgenesis (CCN5 Tg) or AAV9-mediated gene transfer (AAV9-CCN5). The mRNA levels of pro-fibrotic and pro-inflammatory genes were markedly upregulated by AngII infusion, which was significantly normalized by CCN5 overexpression. *In vitro* studies in isolated atrial fibroblasts demonstrated a marked reduction in AngII-induced fibroblast transdifferentiation in CCN5-treated atria. Moreover, while AngII increased the expression of phosphorylated CaMKII and ryanodine receptor 2 levels in HL-1 cells, these molecular features of AF were prevented by CCN5. Electrophysiological studies in *ex-vivo* perfused hearts revealed a blunted susceptibility of the AAV9-CCN5-treated hearts to rapid atrial pacing-induced arrhythmias and concomitant reversal in AngII-induced atrial action potential prolongation. These data demonstrate the utility of a gene transfer approach targeting CCN5 for reversal of adverse atrial structural and electrophysiological remodeling.

Introduction

Atrial fibrillation (AF), the most prevalent arrhythmia in humans, is often accompanied by heart failure (HF). This arrhythmia is associated with the increased risk of stroke, sudden death, and cardiovascular morbidity and mortality [1]. Despite intensive studies spanning over 100 years, a clear understanding of AF mechanisms is still lacking, hampering the development of effective therapeutic approaches that are currently limited to destructive ablation techniques or sub-optimal (and potentially pro-arrhythmic) pharmacotherapy [2-4]. While ablation is effective for treating paroxysmal AF episodes, its utility in the treatment of sustained AF arising in the setting of heart failure is inadequate. Instead, pharmacological approaches are used to achieve either rate or rhythm control. These approaches, however, are mired by extracardiac toxicities and pro-arrhythmic effects, including risk of torsade de pointes and sudden death.

Adverse atrial structural and electrical remodeling are believed to form both the substrate and triggers required for AF initiation and maintenance. Classic anti-arrhythmic approaches targeting individual ion channels have largely failed to prevent AF in structurally remodeled hearts, pointing to the need to address the structural abnormalities that promote AF, namely interstitial fibrosis, myocyte hypertrophy, and myolysis. Of particular importance to the maintenance of AF is the development of interstitial atrial fibrosis that ultimately disrupts cell-to-cell electrical conduction and triggers single/multiple-circuit reentry [5,6]. Fibroblast to myofibroblast trans-differentiation is the key mechanism underlying pro-fibrotic structural remodeling [7]. In addition, defective Ca^{2+} handling is widely believed to mediate the arrhythmic triggers required for AF initiation [8,9]. Specifically, abnormal diastolic Ca^{2+} leak from the sarcoplasmic reticulum (SR) creates a transient inward current (I_{ti}) that produces delayed afterdepolarizations (DADs). In a mouse model, inhibition of Ca^{2+}- and calmodulin-dependent protein kinase II (CaMKII) suppresses hyper-phosphorylation of ryanodine receptor 2 (RyR2) at Ser2814 and aberrant SR Ca^{2+} leak [10].

CCN5 is a member of the CCN family of matricellular proteins (CCN1-6) that shares conserved modular domains, including: (i) insulin-like growth factor-biding domain, (ii) von Willebrand factor type-C domain, (iii) thrombospondin type-1 domain, and (iv) C-terminal cysteine-knot domain [11]. CCN5 is indeed a structurally unique protein that lacks the cysteine-rich C-terminal domain present in other CCN family members. Secreted and matrix-associated CCN5 regulates diverse aspects of cell function, including signaling, adhesion, migration, and proliferation [12]. In previous studies, we identified potent anti-hypertrophic and anti-fibrotic properties of CCN5 in the ventricles of mice that underwent transverse aortic constriction [13].

We further showed that CCN5 overexpression following TAC reverses pre-established ventricular fibrosis by promoting myofibroblast-specific apoptosis [7].

In the present study, the putative role of CCN5 in either preventing or treating adverse atrial remodeling and atrial arrhythmias was investigated in CCN5 overexpressing transgenic (CCN5 Tg) mice as well as mice treated with AAV9-mediated CCN5 gene delivery. We also utilized angiotensin II (AngII) to induce AF in mice. Activation of renin-angiotensin system is thought to play a key role in the development of AF in humans [14]. Accordingly, AngII is widely used to recapitulate the pathogenic scenarios of AF in animal models. Our data demonstrate that CCN5 attenuates AngII-induced atrial interstitial fibrosis, atrial electrical remodeling, and atrial arrhythmia. Moreover, CCN5 modulates phosphorylation of CaMKII and RyR2 in atrial myocytes *in vitro* and inhibits trans-differentiation of atrial fibroblast into myofibroblast *in vitro*. Therefore, these data suggest that CCN5 may be a viable target for the treatment of AF arising in the setting of structural heart disease.

Funding

During this work, D.J. was supported by the assistant Secretary of Defense for Health Affairs endorsed by the Department of Defense, through the FY17, DMDRP, Career Development Award program under Award No. W81XWH-18-1-0322. W.J.P. was supported by grants from National Research Foundation of Korea (2019R1A4A1028534, 2019R1A2C2085457) funded by the Korean Government (MSIP).

Author contributions

W.J.P. and D.J conceptualized and supervised this work. M.-A.L., N.R., M.H.S., J.Y., M.L., S.P.J., T.H.K., H.K., E.-K.C., T.-J.C., R.J.H., D.J. and W.J.P designed the research, performed the experiments, analyzed the data. M.-A.L., N.R., M.H.S., D.J and W.J.P. wrote, revised, and performed a final revision of the manuscript.

Conflict of interests

T.H.K and W.J.P. have co-ownership interest in BethphaGen. The other authors have declared that no conflict of interest exists.